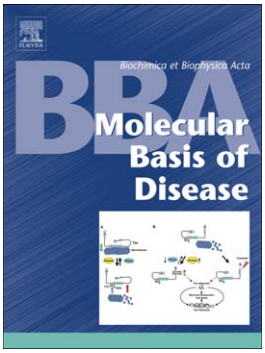

The rescue of microtubule-dependent traffic recovers mitochondrial function in Parkinson's disease

A.R. Esteves, I. Gozes, S.M. Cardoso

PII: S0925-4439(13)00296-2
DOI: doi: 10.1016/j.bbadis.2013.10.003
Reference: BBADIS 63808

To appear in: *BBA - Molecular Basis of Disease*

Received date: 11 June 2013
Revised date: 30 September 2013
Accepted date: 4 October 2013

Please cite this article as: A.R. Esteves, I. Gozes, S.M. Cardoso, The rescue of microtubule-dependent traffic recovers mitochondrial function in Parkinson's disease, *BBA - Molecular Basis of Disease* (2013), doi: 10.1016/j.bbadis.2013.10.003

The rescue of microtubule-dependent traffic recovers mitochondrial function in Parkinson's disease

Esteves AR[1], Gozes I[2], Cardoso SM[1,3]

[1]CNC–Center for Neuroscience and Cell Biology, University of Coimbra; [2]Department of Human Molecular Genetics and Biochemistry, Sagol School of Neuroscience, Adams Super Center for Brain Studies, Sackler Faculty of Medicine, Tel Aviv University, Tel Aviv, Israel; [3]Faculty of Medicine, University of Coimbra, Coimbra, Portugal.

*Corresponding author: Sandra Morais Cardoso, CNC - Center for Neuroscience and Cell Biology, University of Coimbra, Largo Marquês de Pombal 3004-517 Coimbra, Portugal; Phone: +351 239 820190; Fax: +351-239-822776; E-mail: cardoso.sandra.m@gmail.com

Conflict of interest: I. Gozes is a Director-Chief Scientific Officer at Allon Therapeutics Inc. the company that develops davunetide (NAP).

Abstract

In Parkinson's disease mitochondrial dysfunction can lead to a deficient ATP supply to microtubule protein motors leading to mitochondrial axonal transport disruption. Compromised axonal transport will then lead to a disorganized distribution of mitochondria and other organelles in the cell, as well as, the accumulation of aggregated proteins like alpha-synuclein. Moreover, axonal transport disruption can trigger synaptic accumulation of autophagosomes packed with damaged mitochondria and protein aggregates promoting synaptic failure.

We previously observed that neuronal-like cells with an inherent mitochondrial impairment derived from PD patients contain a disorganized microtubule network, as well as, alpha-synuclein oligomers accumulation. In this work we provide new evidence that an agent that promotes microtubule network assembly, NAP (davunetide), improves microtubule-dependent traffic, restores the autophagic flux and potentiates autophasosome-lysosome fusion leading to autophagic vacuole clearance in Parkinson's disease cells. Moreover, NAP is capable of efficiently reduce alpha-synuclein oligomer content and its sequestration by the mitochondria. Most interestingly, NAP decreases mitochondrial ubiquitination levels, as well as, increases mitochondrial membrane potential indicating a rescue in mitochondrial function.

Overall, we demonstrate that by improving microtubule-mediated traffic, we can avoid mitochondrial-induced damage and thus recover cell homeostasis. These results prove that NAP may be a promising therapeutic lead candidate for neurodegenerative diseases that involve axonal transport failure and mitochondrial impairment as hallmarks, like Parkinson's disease and related disorders.

Keywords: NAP, mitochondria dynamics, microtubule network

Abbreviations:

PD, Parkinson's disease; ASYN, alpha-synuclein; CT cybrids (control cybrids); sPD cybrids (sporadic Parkinson's disease cybrids); mtDNA, mitochondrial DNA; MPP^+, 1-methyl-4-phenylpyridinium.

1. Introduction

There is accumulating evidence from *in vitro* and *in vivo* studies suggesting that mitochondrial abnormalities are a common event in sporadic Parkinson's disease (sPD) **[1-4]**. Moreover, defects in axonal and dendritic transport have also been linked to various neurodegenerative processes, including sPD pathogenesis. Indeed, sPD is characterized by a sequence of neuropathological events that arise due to a dying-back pattern of neuronal degeneration, namely early loss of synaptic terminals and axonopathy, before cell death **[5-8]**. Another central hallmark of PD is the presence of intracytoplasmatic aggregates, named Lewy Bodies that are mainly composed of alpha-synuclein (ASYN). Several studies suggest that larger ASYN aggregates may have reduced toxicity relative to their smaller-sized counterparts, the soluble oligomers **[9-12]**. ASYN inclusion dynamics results from an intricate process that may distress axonal transport, autophagic-lysosomal and ubiquitin-proteasome pathways.

Mitochondrial function and axonal transport are intimately connected. Mitochondria supply the energy for cytoskeleton motor proteins to transport them along cytoskeleton tracks to areas in the cell where energy demands are high and calcium buffering is required **[13, 14]**. Importantly, alteration in microtubule dynamic may lead to a defective traffic of mitochondria inside the cell contributing ultimately to its dysfunction and to the disruption of protein transport, such as ASYN. ASYN, which is normally transported by fast axonal transport, can then accumulate potentiating the disruption of intracellular traficking **[15]**.

Since mitochondria are metabolically and functionally compromised in PD tissues it is important to evaluate mitochondrial contribution to microtubule transport failure. Axonal transport requires energy to allow molecular motors to move along microtubules and transport mitochondria, autophagic and synaptic vesicles **[16]**. Recently, Zala and co-workers [17] challenged the assumption that mitochondrial ATP was the principal source of energy for motor molecules. They showed that the transport of BDNF carrying vesicles were not affected by the inhibition of mitochondrial ATP production, but failed to demonstrate the same for mitochondrial transport, which is dependent on the hydrolysis of mitochondrial ATP by molecular motors.

In previous work we observed that sPD cybrids contain mitochondrial abnormalities, such as a complex I defect and ATP depletion. **[18-20]**. This *ex-vivo* model results from the fusion of teratocarcinoma (NT2) cells that were depleted from their mitochondrial DNA (mtDNA) (NT2 rho0) with mitochondria isolated

from platelets of age-matched healthy individuals or PD patients. Indeed, we and others claim that the differences observed in the mitochondrial pool between CT and PD cybrids are due to mtDNA variations. Although we agree that there is no demonstrated homoplasmic mtDNA mutation that associates with PD, we cannot rule out the presence of low abundance heteroplasmic mutations, epigenetic modifications to the mtDNA, or the possibility that polymorphic variation (rather than mutations *per se*) are responsible for the observed biochemical phenotypes. mtDNA polymorphic variation between individuals is high, which suggests mtDNA between cybrid lines containing mtDNA from different individuals is certainly different. The great potential of this model is that these cells possess the same nuclear background but different mitochondrial background therefore allowing us to study mitochondrial role in several cellular pathways **[21]**. We also demonstrated that sPD cybrids present basal microtubule disruption with a concomitant accumulation of ASYN oligomers **[22]**. Hence, we showed that microtubule network alterations are due to mitochondrial deficits. We further proved that taxol, a known microtubule stabilizer, promoted microtubule network assembly and a decrease in ASYN oligomers content **[22]**. However, taxol is not neuron-specific, has limited brain bioavailability and in high concentration has the capacity to inhibit microtubule dynamics **[23]**. Thus, more specific, brain-penetrable microtubule-interacting drugs are required **[24]**. Herein, we decided to use a peptide known as NAP (davunetide) that is an eight amino acid peptide derived from an activity-dependent neuroprotective protein **[25-27]**. This peptide associates with tubulin and enhances proper microtubule assembly **[28-30]**. We demonstrate that the alterations induced by mitochondrial deficits on microtubule assembly and microtubule-mediated traffic in sPD cybrids are prevented by NAP. Correlated with this we observed that NAP promoted autophagic vacuoles clearance by increasing autophagic flux and autophagossome-lysosome fusion in PD cells. Moreover, NAP restored mitochondrial distribution and mitochondrial membrane potential and was able to prevent the accumulation of Triton-soluble and insoluble ASYN oligomeric species in sPD cybrids.

Taken collectively, our results provide strong data that NAP is a promising therapeutic agent in the PD treatment.

2. Material and Methods

2.1 Chemicals

Nocodazole, MPP^+ (1-methyl-4-phenylpyridinium), ammonium chloride (NH_4Cl), Leupeptin, Oligomycin, Carbonyl cyanide-p-trifluoromethoxyphenylhydrazone (FCCP), Rapamycin, Ubiquinone and Rotenone were obtained from Sigma (St. Louis, MO, USA). Rhodamine 123 was purchased from Molecular Probes (Eugene, OR, USA). NAP was generously donated by Dr. Illana Gozes from Tel Aviv University.

2.2 Human subjects

Subject participation was approved by the University of Kansas School of Medicine's Institutional Review Board. The mean age of the PD subjects (n=9) who participated in this study was 64 ± 12.8 years, and for the control subjects (n=5) it was 74.3 ± 5.5 years (supplementary Table I). The PD subjects were followed regularly in a tertiary referral movement disorders clinic at the Kansas University Medical Center and met current criteria used to diagnose idiopathic PD in clinical and research settings **[31]**. The control subjects were participants of a longitudinal "normal aging" cohort that is characterized serially by the Brain Aging Program at the University of Kansas School of Medicine (see supplementary Table I). After obtaining informed consent, sporadic PD and age-matched control subjects underwent a 10 ml or 60 ml phlebotomy using tubes containing acid-citrate-dextrose as an anticoagulant. The control subjects had no evidence of a neurodegenerative condition.

2.3 Preparation of platelet mitochondria

Following provision of informed consent, 60 ml of blood was collected through venipuncture in tubes containing acid–citrate–dextrose as an anticoagulant. Mitochondria were obtained from human platelets according to previously described methods **[32]**. Platelet mitochondria protein concentrations were measured by the Bradford protein assay **[33]**, in which bovine serum albumin was used as the standard.

2.4 Creation of cybrid cell lines

To create the cybrid cell lines for this study, we used NT2 (Ntera2/D1) cells, a teratocarcinoma cell line with neuronal characteristics (Stratagene, La Jolla, CA) **[34, 35]**. These cells were depleted of endogenous mtDNA (NT2 rho0 cells) via long-term ethidium bromide exposure **[36, 37]**. NT2 rho0 cells lack intact mtDNA, do not possess a functional electron transport chain, and are auxotrophic for pyruvate and uridine **[38]**. Consequently, platelet mitochondria from either PD or control subjects were isolated from the individual blood samples and were used to repopulate NT2 rho0 cells with mtDNA as previously described **[36, 37]**. We generate control and disease cell lines at the same point in time and only compared a disease series with a control series that had been made at the same time and with the same immediate stock of NT2 rho0 cells. Briefly, NT2 rho0 cells were co-incubated in Polyethylene glycol (Merck Chemicals) with platelets from the human subjects **[38]**. After that the resulting mixture was grown in Rho0 medium in T75 flasks. Seven days after plating, untransformed cells were removed by withdrawal of pyruvate and uridine from the culture medium and substitution of dialyzed, heat inactivated fetal calf serum for non-dialyzed, heat inactivated fetal calf serum **[39, 21]**. Maintaining cells in selection medium removes rho0 cells that have not repopulated with platelet mtDNA. Moreover, "mock fusions" in which NT2 rho0 cells were not incubated with platelets were plated and maintained in selection medium in parallel with the true fusions. During the selection period all cells from the mock fusions died. After

selection was complete, the resultant cybrid cells were switched to cybrid growth medium. Cells were grown in 75 cm^2 tissue culture flasks maintained in a humidified incubator at 37ºC and 5% CO_2.

2.5 Cell line culture and experimental treatments

Optimem and Dulbeco's modified Eagle's medium (DMEM) were obtained from Gibco-Invitrogen (Life Technologies Ltd, UK). Non-dialyzed and dialyzed Fetal Bovine Serum (FBS) was obtained from Gibco-Invitrogen (Life Technologies Ltd, UK). NT2 rho0 cell growth medium Optimem was supplemented with 10% non-dialyzed FBS, 200 µg/ml sodium pyruvate from Sigma (St. Louis, MO, USA), 100 µg/ml uridine from Sigma (St. Louis, MO, USA) and 1% penicillin-streptomycin solution. NT2 Cybrid selection medium consisted of DMEM supplemented with 10% dialyzed FBS and 1% penicillin-streptomycin solution. Cybrid growth medium consisted of Optimem supplemented with 10% non-dialyzed FBS and 1% penicillin-streptomycin solution. Prior to experiments, cell lines were maintained in the cybrid growth medium. For Western blotting analysis and mitochondrial respiratory chain complex I activity, cybrid cell lines were seeded in petri-dishes at a density of $0.5x10^6$ cells/well. For immunoblotting analysis, cybrid cell lines were grown on coverslips in 12-well plates at a density of $0.1x10^6$ cells/well. For Live Imaging analysis, cybrid cell lines were grown on µ-slide 8-well plates from ibidi at a density of $0.06x10^6$ cells/well. For mitochondrial membrane potential measurements, cybrid cell lines were grown on 24-well plates at a density of $0.075x10^6$ cells/well. After 24h experimental treatments were performed. NAP was prepared in water and was added for 24h to the culture medium with a final concentration of 1 nM. Where indicated, 0.5 µM Rapamycin, 20 mM NH_4Cl and/or 100 µM Leupeptine (Sigma, St. Louis, MO, USA), were added for 4h to the culture medium. The combination of NH_4Cl with Leupeptine blocks all types of autophagy, as it reduces the activity of all lysosomal proteases by increasing the lysosomal lumen pH without affecting the activity of other intracellular proteolysis systems **[40]**. Rapamycin is an mTOR inhibitor that induces autophagy.

2.6 Animals

Experiments involving animals were approved by and performed in accordance with University of Coimbra Institutional Animal Care and Use Committee guidelines and European Community Council Directive for the Care and Use of Laboratory Animals (86/609/ECC).

2.7 Primary cortical neuronal cultures and experimental treatments

Neurobasal medium and B27 supplement were purchased from Gibco BRL, Life Technologies (Scotland, UK). Trypsin, Trypsin inhibitor type II-S-soybean and bovine serum albumin (BSA) were obtained from Sigma (St. Louis, MO, USA). Primary cultures of cortical neurons were prepared from 15 to 16 days embryos of Wistar rats according to the method described by Yu and collaborators **[41]** , with some

modifications **[42]**. Briefly, removed cortices were aseptically dissected and placed in Ca^{2+} and Mg^{2+}-free Krebs buffer: 120.9 mM NaCl, 4.8 mM KCl, 1.2 mM KH_2PO_4, 13 mM glucose and 10 mM HEPES (pH 7.4) supplemented with BSA (0.3 mg/mL). Cortical tissues were then washed and incubated in Krebs solution supplemented with BSA, and containing trypsin (0.35 mg/mL) for 10 min at 37°C. The tissue digestion was subsequently stopped with the addition of Krebs buffer containing trypsin inhibitor (type II-S) (0.75 mg/mL), followed by a centrifugation at 140 × g for 5 min. After washing the pellet once with Krebs buffer, the cells were resuspended in fresh Neurobasal medium supplemented with 0.2 mM L-glutamine, 2% (v/v) B27 supplement, penicillin (100 U/mL) and streptomycin (100 µg/mL) and were dissociated mechanically. For Western Blotting analysis cortical neurons were seeded on poly-L-lysine (0.1 mg/mL) coated 6-well plates at a density of 1.6×10^6 cells/mL. For immunoblotting analysis, cortical neurons were seeded on poly-L-lysine (0.1 mg/mL) coated coverslips at a density of 0.75×10^6 cells/mL. The cultures were maintained in serum-free Neurobasal medium supplemented with B27, at 37°C in a humidified atmosphere of 5% CO_2 and atmosphere of 5% CO_2/95% air for 5–7 days before treatments in order to allow neuronal differentiation. After 5 to 7 days in vitro, cells were incubated for 24h with MPP^+ (Sigma, St. Louis, MO, USA) freshly prepared in water with a final concentration of 100 µM and when indicated with NAP prepared in water with a final concentration of 10 nM. In autophagic flux experiments 20 mM NH_4Cl and 20 µM Leupeptine (Sigma, St. Louis, MO, USA), were added 4h before NAP and/or MPP^+ treatment ended. For all experimental procedures, controls were performed in the absence of those agents.

2.8 Preparation of cell extracts containing soluble and polymeric tubulin

To prepare the soluble and polymeric fractions of cell tubulin, cells were washed twice very gently with a microtubule stabilizing buffer (0.1 M N-morpholinoethanesulfonic acid, pH 6.75, 1 mM $MgSO_4$, 2 mM EGTA, 0.1 mM EDTA, 4 M glycerol). Soluble proteins were extracted at 37°C for 6 min in 100 µL of microtubule stabilizing buffer containing 1% Triton X-100. The remaining fraction in the culture dish was scrapped in 100 µL of 25 mM Tris (pH 6.8), 0.1% SDS, and frozen three times in liquid nitrogen **[43]**. Protein was quantified by the Bio-Rad protein dye assay reagent (Bio-Rad, Hercules, CA, USA).

2.9 Preparation of mitochondrial and cytosolic extracts

To perform mitochondrial and cytosolic fractions, cells were washed with Phosphate-buffered solution (PBS), scraped in a buffer containing 250 mM sucrose, 20 mM Hepes, 1 mM EDTA, 1 mM EGTA, supplemented with protease inhibitors (0.1 M phenyl-methylsulfonyl fluoride (PMSF) from Sigma (St. Louis, MO, USA), 0.2 M dithiothreitol (DTT) from Sigma (St. Louis, MO, USA), and 1:1000 dilution of a protease inhibitor cocktail and subsequently homogenized. Then cells are centrifuged at 492 × g for 12 min at 4ºC. The resulting supernatant was centrifuged at 11,431 × g for 20 min at 4ºC. Pellets resulting from this step constitute a crude mitochondrial fraction and the supernatants corresponded to the cytosolic fraction. The cytosolic fraction was then precipitated with TCA 5% and consequently centrifuged at

15,643 × g for 10 min at 4ºC. The resulting pellet was resuspended in sucrose buffer and was then neutralized with 2.5 M KOH pH 7. Subsequently cytosolic and mitochondrial fractions were frozen three times on liquid nitrogen. Protein was quantified by the Bio-Rad protein dye assay reagent (Bio-Rad, Hercules, CA, USA).

For ASYN oligomers, LC3, acetylayted α-tubulin levels determination cytosolic cell extracts were prepared as followed. Individual cell lines were washed in ice-cold PBS (1x) and lysed in 1% Triton X-100 containing hypotonic lysis buffer (25 mM HEPES, pH 7.5, 2 mM $MgCl_2$, 1 mM EDTA and 1 mM EGTA supplemented with 2 mM DTT, 0.1 mM PMSF and a 1:1000 dilution of a protease inhibitor cocktail from Sigma. Cell suspensions were frozen three times in liquid nitrogen and centrifuged at 20,000 × g for 10 min. The resulting supernatants were removed and stored at -80ºC. For the analysis of ASYN oligomers, the supernatants (Triton-soluble fractions) were collected and saved and the pellets (Triton-insoluble fractions) were resuspended in 1× specific sample buffer (0.2 M Tris-HCl, pH 6.8, 40% glycerol, 2% SDS, 0.005% Coomassie). Protein content was determined using Bio-Rad protein dye assay reagent (Bio-Rad, Hercules, CA, USA).

2.10 Live imaging

After treatment cells were washed with Hanks' balanced salt solution (HBSS) and incubated with 100 nM MitoTracker green (Invitrogen, Carlsbad, CA) for 30 min at 37ºC in the dark to label mitochondria **[44]**. After incubation cells were carefully washed twice and kept in HBSS. The cells were then imaged for mitochondrial movements. An organelle was considered to be no mobile if it remained stationary for the entire recording period. Movement was counted only if the displacement was more than the length of the mitochondrion (about 2 μm). Time-lapse images were captured under a Zeiss LSM 510 meta confocal microscope with a stage-based chamber (5% CO_2, 37 °C). The inverted microscope was driven by LSM software. Images were taken every 2 s for a total of 4 min under 63× magnification (Zeiss Plan-ApoChromat 63x, 1.4NA). For each time-lapse movie, mitochondria were manually tracked and transport parameters of mitochondria movements were generated using the ImageJ software plug-in Multiple Kymograph, submitted by J. Rietdorf and A. Seitz (European Molecular Biology Laboratory, Heidelberg, Germany). Mitochondrial movement velocity data were determined from the kymographic images and were calculated based on the slope (v=dx/dt) obtained for each mitochondrion movement profile along the recording time. Mitochondria were considered stationary if they did not move more than 2 μm during the entire recording period. Each series of images was recorded for at least three randomly selected Mitotracker Green labeled cells per culture and 3 independent cultures per condition.

2.11 Immunocytochemistry and confocal microscopy analysis

After treatment cells were washed twice with PBS 1x and fixed for 30 min at room temperature using 4% paraformaldehyde. The fixed cells were washed again with PBS 1x three times and permeabilized with 0.2% Triton X-100 for 2 min. Subsequently cells were washed three times with PBS 1x and blocked with

3% BSA for 30 min. Cells were then washed again three times with PBS 1x and then incubated with primary antibody (1:2,000 monoclonal anti-α-tubulin from Sigma (St. Louis, MO, USA) for 1 h; 1:100 polyclonal anti-Tom20 from Santa Cruz Biotechnology (Santa Cruz, CA., USA) overnight; 1:2,000 monoclonal anti-acetylated-α-tubulin from Sigma (St. Louis, MO, USA) for 1 h; 1:200 polyclonal anti-LC3B from Cell Signaling (Danvers, MA, USA) overnight; 1:400 rabbit monoclonal anti-LC3 XP® from Cell Signaling (Danvers, MA, USA); 1:100 anti-LAMP-1 clone H4A3 from the Developmental Studies Hybridoma Bank (University of Iowa, Iowa City, IA, USA) overnight; monoclonal anti-βIII-Tubulin from Cell Signaling (Danvers, MA, USA) overnight) and then with the appropriate secondary antibody 1:250 alexa fluor 594 or 1:250 alexa fluor 488 from Molecular Probes (Eugene, OR, USA). After that cybrid cell lines were incubated with Hoescth 15 µg/µL for 5 min at RT and protected from light. Cells were then washed twice in PBS and the coverslips were immobilized on a glass slide with mounting medium DakoCytomation (Dako, Glostrup, Denmark). Images were acquired on a Zeiss LSM510 META confocal microscope (63× 1.4NA plan-apochromat oil immersion lens) by using Zeiss LSM510 v3.2 software (Carl Zeiss Inc., Thornwood, NY, USA) and analyzed using Zeiss LSM Image Examiner. The number of LC3 dots per cell was quantified using the "analyze particle" function of the ImageJ v1.39k (National Institute of Health, USA) program. As previously described by Dagda and colleagues **[45]**, to quantify two parameters of mitochondrial morphology an ImageJ macro was used. The cells stained with Tom20 were extracted to grayscale, inverted to show mitochondria-specific fluorescence as black pixels and thresholded to optimally resolve individual mitochondria. This macro traces mitochondrial outlines using "analyze particles". The area/perimeter ratio was employed as an index of mitochondrial interconnectivity and inverse roundness was used as a measure of mitochondrial elongation. Co-localization between LC3XP/Lamp-1 was quantified in tresholded images with the JACoP plug-in of the ImageJ software, according to Bolte and Cordelières **[46].**

2.12 Western blot analysis

For the analysis of ASYN oligomers, both fractions (Triton-soluble and insoluble) were loaded onto 12% SDS-PAGE under non-reducing and non-denaturating conditions. For the analysis of free and polymerized α-tubulin, acetylated α-tubulin, LC3B and cytosolic and mitochondrial ASYN, the samples were resuspended in 6x sample buffer (4x Tris.Cl/SDS, pH 6.8, 30% glycerol, 10% SDS, 0,6 M DTT, 0.012% bromophenol blue). Free and polymerized α-tubulin, as well as, acetylated-α-tubulin samples were loaded onto 10% SDS-PAGE, LC3B samples were loaded onto 15% SDS-PAGE, ASYN cytosolic and mitochondrial samples were loaded onto 12% SDS-PAGE. All these samples were loaded under reducing conditions. After transfer to PVDF membranes (Millipore, Billerica, MA, USA), the membranes were incubated for 1h in Tris-Buffered Solution (TBS) containing 0.1% Tween 20 and 5% nonfat milk, followed by an overnight incubation with the respective primary antibodies at 4ºC with gentle agitation: 1:100 monoclonal anti-ASYN LB509 from Zymed Laboratories Inc. (South San Francisco, CA, USA); 1:1,000 polyclonal anti-LC3B from Cell Signaling (Danvers, MA, USA); 1:16,000 monoclonal anti-acetylated α-tubulin from Sigma (St. Louis, MO, USA); 1:500 polyclonal anti-ubiquitin from Santa Cruz Biotechnology (Santa Cruz, CA, USA). 1:10,000 monoclonal anti-α-Tubulin from Sigma (St. Louis, MO,

USA) was used for the analysis of free/polymerized α-Tubulin and for loading control. 1:500 monoclonal anti-GAPDH from Millipore (Billerica, MA, USA) and 1:100 polyclonal anti-Tom20 from Santa Cruz Biotechnology (Santa Cruz, CA, USA) were also used for loading control. 1:500 anti-DAT (H80) Santa Cruz Biotechnology (Santa Cruz, CA, USA) were also used to validate primary cultures of cortical neurons as a model to study MPP^+-induced toxicity. Membranes were washed with TBS containing 0.1% non-fat milk and 0.1% Tween three times (each time for 10 min), and then incubated with the appropriate horseradish peroxidase-conjugated secondary antibody for 2 h at room temperature with gentle agitation. After three washes specific bands of interest were detected by developing with an alkaline phosphatase enhanced chemical fluorescence reagent (ECF from GE Healthcare, Piscataway, NJ, USA). Fluorescence signals were detected using a Biorad Versa-Doc Imager, and band densities were determined using Quantity One Software.

2.13 Analysis of mitochondrial membrane potential (Δψm) with rhodamine 123 probe

To monitor changes in mitochondrial membrane potential Rhodamine 123 probe (Rh123) (Molecular Probes, Eugene, OR, USA) was used. Rh123 is a fluorescent cationic dye that distributes electrophoretically into the mitochondrial matrix in response to the electrical potential across the inner mitochondrial membrane. The accumulation in functional mitochondria takes place as a consequence of Rh123 positive charge; thereby a decrease in Rh123 cellular retention is associated with a decrease in Δψm. After treatments cells were washed with PBS (1x) and subsequently loaded in the dark with 1 μM Rh123 in Krebs buffer (pH 7.4) composed of 132 mM NaCl, 4 mM KCl, 1.4 mM $MgCl_2$, 6 mM Glucose, 10 mM HEPES, 10 mM $NaHCO_3$, 1 mM $CaCl_2$. Basal Fluorescence was recorded for 45 min at 37ºC (λex=552 nm and λem=581 nm). Afterwards 1 μM FCCP (protoionophore) and 2 μg/mL oligomycin (inhibitor of H+ transporting ATP synthase and an inhibitor of Na+/K+ transporting ATPase) were added to each well in order to achieve maximal mitochondrial depolarization and to prevent ATP synthase reversal, respectively. Measurements were recorded for another 15 min at 37ºC. Rh123 retention ability was calculated by the difference between the total fluorescence (after depolarization) and the initial value of fluorescence (basal fluorescence). Results are expressed as a percentage of the dye retained within the untreated CT cybrids. Measurements were performed using a Spectramax Plus 384 spectrofluoremeter (Molecular Devices, Sunnyvale, CA, USA).

2.14 MTT cell proliferation assay

Cell proliferation was determined by the colorimetric MTT (3-(4,5- dimethylthiazol-2-yl)-2,5-diphenyltetrazolium bromide) assay **(Mosmann, 1983)**. In viable cells, MTT is metabolized into a formazan that absorbs light at 570 nm. Following the cell treatment protocol the medium was aspirated and 0.5 ml MTT (0.5 mg/ml) was added to each well. The plate was then incubated at 37 °C for 3 h. At the end of the incubation period the formazan precipitates were solubilized with 0.5 ml of acidic isopropanol (0.04MHCl/isopropanol). The absorbance was measured at 570 nm. Cell reduction ability was expressed as a percentage of the untreated neurons.

2.15 Data analysis

All data result from the analysis of duplicates per experimental condition in at least three independent experiments and are expressed as the mean ± SEM. Statistical analyses were performed using GraphPad Prism 5 (GraphPad Software, San Diego, CA, USA). Differences between two data sets were evaluated by two tailed unpaired Student's *t*-test. Statistical tests between multiple data sets and conditions were carried out using a one way analysis of variance (ANOVA) with pair-wise multiple comparison procedures using the post hoc Bonferroni's test to determine statistical significance, as appropriate. A p-value<0.05 was considered statistically significant.

3. Results

3.1 NAP rescues mitochondrial-mediated microtubule network disruption

Microtubules assembly requires a balanced equilibrium between polymerized and unpolymerized tubulin. We assessed NAP (1 nM) effect on microtubule network through immunoblotting and measurement of the levels of free and polymerized α-tubulin. We observed that NAP significantly decreased the ratio between free and polymerized tubulin in sPD cybrids comparatively to untreated sPD cybrids ($p < 0.001$) (**Fig.1A**), and induced the formation of tubulin bundles similar to those observed in untreated CT cybrids cells (**Fig. 1B**). Subsequently we evaluated α-tubulin acetylation levels, since this post-translational modification is a marker of stable microtubules **[47]**. Interestingly, NAP promoted a significant increase in α-tubulin acetylation levels in sPD cybrids indicating that it promotes microtubule stability ($p < 0.05$) (**Fig. 1C**). These results were confirmed by immunocytochemistry analysis of acetylated-α-tubulin levels showing that sPD cybrids harbour less acetylated-α-tubulin levels and that NAP promoted an increase in the acetylation of α-tubulin.

In order to prove that NAP targets the microtubule system we quantitatively evaluated whether NAP prevented the disruption of the microtubule network promoted by nocodazole. We observed that NAP prevented microtubule depolymerisation induced by nocodazole (**Figs S1A, B**), decreasing the ratio between free and polymerized α-tubulin and increasing acetylated α-tubulin levels ($p < 0.01$). Interestingly, despite nocodazole induced an overall decrease in the levels of acetylated α-tubulin **(Fig S1B)** it also induced the formation of acetylated α-tubulin knots in both CT and sPD cybrids (Data not shown). These results corroborate and extend previous observation in primary cultures derived from rat cerebral cortex **[48]**.

3.2 NAP positively affects mitochondrial trafficking

Mitochondrial long-distance transport, to reach all the places that need energy, is mainly mediated by motor proteins powered by ATP hydrolysis that shuttle mitochondria along microtubules **[49]**. We have shown earlier that mitochondrial deficits induce alterations in microtubule network, mainly characterized

by an increase in free/polymerized tubulin ratio **[50]** and by an impairment of mitochondrial trafficking **[40]**. In order to determine if NAP could improve intracellular trafficking we recorded whether mitochondria moved or remained static (**Fig. 2A**), and subsequently the moving mitochondria velocity (**Fig. 2B**) and the relative number of stationary or movable events was calculated (**Fig. 2C**), as previously described **[40]**. Accordingly to our previous results, average mitochondrial velocities were decreased in sPD cybrids. As expected, NAP promoted an increase in moving mitochondria velocity in sPD cybrids (**Fig. 2B**), despite no significant change is reached. As shown in **Fig. 2C**, sPD cybrids exhibited a significant decreased number of movable mitochondria in the studied fields. In addition, NAP was able to reestablish the number of movable mitochondria in sPD cybrid cells. Altogether, our data suggest that promoting the dynamic stability and functional integrity of microtubule network allows mitochondrial motility.

3.3 NAP restores microtubule dependent traffic allowing macroautophagy completion

Autophagic flux is highly dependent on microtubule network. In fact, microtubules have been implicated in the initiation and maturation of autophagosomes, serve as tracks for movement of mature autophagosomes and bring autophagosomes and lysosomes together for fusion and disposal of autophagosomal cargo **[51, 52]**. Therefore, we decided to explore NAP effects on the autophagic pathway in our cellular model, since previous data showed that LC3II levels are increased in sPD cybrids when compared to CT cybrids indicating that sPD cybrids either harbour decreased autophagosomal biogenesis or decreased autophagosomal degradation **[40]**. To address this question we monitored the autophagic flux, the process from autophagosome formation to degradation, comparing the accumulation of autophagosomes after inhibition of lysosomal function (with NH_4Cl and leupeptin) to the steady-state levels. Interestingly, when we treated cells with NAP, LC3II content decreased ($p < 0.01$) (**Fig. 3A**) and the autophagic flux increased in sPD cybrids compared to untreated sPD cybrids (**Fig. 3B**) ($p < 0.001$). Additionally, these data were corroborated by LC3B staining where we observed a reduction in the number of LC3B dots in NAP-treated sPD cybrids when compared to untreated sPD cybrids (**Fig. 3C, D**). Remarkably, NAP by modulating microtubule-dependent traffic of autophagosomes was effective in promoting autophagy turnover in sPD cybrids, as reflected by decreased autophagosome content and improved autophagic flux. These findings suggest that the dynamic interaction of autophagic vacuoles with the microtubule system tracks are altered in sPD cybrids, which obstructs autophagosome transport and so the fusion with lysosome. Autophagosome-lysosome fusion can be visualized via immunofluorescence imaging as the co-localization of LC3B positive vesicles with a lysosome marker (e.g., LAMP-1) **[53]**. We observed a decreased degree of co-localization between LC3B positive vacuoles and Lamp-1 positive vacuoles in sPD cybrids, an effect that was reversed by NAP treatment (**Fig. 3E, F**). This result indicates that macroautophagy is not concluded in sPD cybrids due to a disruption in the autophagosomal intracellular traffic and not to an impairment of autophagosome-lysosome fusion. As a control we used a known autophagic inducer (rapamycin) and found that in sPD cybrids rapamycin did not improve autophagic flux indicating that although autophagy is being induced, sPD cybrids are unable to efficiently proceed with the pathway probably due to vesicular traffic impairment (**Fig. S2**).

Similarly to autophagosomes, ASYN is actively transported by microtubules from its site of synthesis in the cell body along axons to synaptic termini. Several data indicated that defective axonal transport of ASYN is a potential pathogenic event in alpha-synucleinopathies **[54, 55]**. We observed that NAP significantly reduced both ASYN Triton-soluble low weight oligomers and Triton-insoluble high weight oligomers accumulation ($p < 0.05$) (**Fig.S3**). These findings suggest that NAP by improving microtubule-dependent traffic additionally improves autophagic efficiency to clear specific substrates such as aggregated ASYN or/and reduces ASYN propensity to oligomerize.

3.4 Mitochondrial function recovers after NAP treatment

Our next goal was to evaluate NAP effect on mitochondria dynamics and function. We previously observed that NAP improved mitochondrial trafficking (**Fig. 2**) therefore we first addressed mitochondrial distribution, elongation and interconnectivity by using Tom20 antibody staining **[56-61]**. Tom 20 is a subunit of the TOM (translocase of outer membrane) receptor complex responsible for the recognition and translocation of cytosolically synthesized mitochondrial pre-proteins **[62]**. We visualized that in sPD cybrids mitochondrial distribution was more perinuclear than in CT cybrids which is in agreement with the impairment in mitochondrial trafficking (**Fig. 4A**). Interestingly, we observed a decrease in the mitochondrial network in sPD cybrids relatively to CT cybrids, which was reverted after NAP exposure. In fact, NAP improved mitochondrial interconnectivity in sPD cybrids (**Fig. 4B**). Mitochondrial interconnectivity is calculated as the mean area/perimeter ratio and is consistent with the degree of mitochondrial branching, namely the connectivity/dynamics between mitochondria. Worthy of notice is that in NAP-treated cybrids mitochondria seemed more elongated than in untreated cybrids (**Fig. 4A, C**). On the other hand, nocodazole exposure increased mitochondrial fragmentation in sPD cybrids and in both cybrids decreased mitochondrial elongation (**Fig. 4A, C**).

We next assessed mitochondrial function after NAP treatment. Consistent with our previous data we observed a loss of mitochondrial membrane potential in sPD cybrids comparatively to CT cybrids ($p < 0.05$) (**Fig. 4D**) **[18]**. Recent work has shown that parkin selectively and rapidly translocates from the cytosol to depolarized mitochondria, where it mediates the ubiquitination of mitochondrial substrates, such as, voltage-dependent anion-selective protein 1 (VDAC1) and mitofusin1 and 2 **[63-65],** promoting mitochondrial fission. Therefore an increase in mitochondrial ubiquitination can also indicate that mitochondria are being fragmented in order to be targeted for degradation (mitophagy). Correlated with a decrease in mitochondrial membrane potential we also observed an increase in mitochondrial protein ubiquitination levels in sPD cybrids (**Fig. 4E**). By improving microtubule stability, and promoting macroautophagy completion, NAP restored sPD cybrids mitochondrial membrane potential and decreased the presence of mitochondrial ubiquitinated proteins ($p < 0.05$ and $p < 0.001$, respectively) (**Fig. 4D, E**). We also examined mitochondrial ASYN sequestration since several reports have confirmed ASYN localization into the mitochondria **[66-68]**. We detected an increase in ASYN mitochondrial accumulation in sPD cybrids relatively to CT cybrids, which was reduced by NAP treatment (**Fig. 4F**). Our results

support the idea that NAP, by promoting autophagic vacuole clearance, allows the elimination of damaged mitochondria and maintains the pool of healthy mitochondria.

3.5 The MPP^+ model: verification of the results

To extend the above findings and further confirm our previous observation that mitochondrial deficits can compromise the degradative ability of the autophagic system, we used primary cortical neurons treated with MPP^+, an *in vitro* model of PD, which associates neuronal dysfunction with mitochondrial and microtubule impairments **[69, 70]**. We show that primary cortical neurons (rat embryo neocortex) express dopamine transporter (DAT) (**SFig.4A**) and that MPP^+ reduces mitochondrial dehydrogenases activity (**SFig.4B**) and induces a decrease in mitochondrial membrane potential in neurons (**SFig.4C**). Nevertheless, it was also demonstrated that MPP^+ directly impaired microtubules in neuronal cells **[70]**. In our model, we have also found a decrease in α-tubulin acetylation levels ($p < 0.01$) that was slightly prevented by NAP (10 nM) treatment (**Fig. 5A**). Moreover, in this acute model we have also found a rapid accumulation of LC3II within 4 h after blocking of lysosomal proteolysis, indicating a constitutive autophagic flux in primary cortical neurons (**Fig. 5B**). However, we could not observe an increase in the number of LC3II in MPP^+-treated cells when compared to control cells (**Fig.5B**), although this was accompanied by a significant reduction on the autophagic flux ($p < 0.01$) (**Fig. 5B, C**), similarly to the results obtained in sPD cybrids. NAP was able to restore the autophagic flux impaired by MPP^+-treatment ($p < 0.05$) (**Fig. 5B, C**). βIII-Tubulin staining also indicated a decrease in the length and number of neuronal processes after MPP^+ exposure that are restored by NAP treatment, indicating an increase in neuronal viability and plasticity. Moreover, MPP^+-treated neurons show a less distributed mitochondrial network when compared to untreated neurons (**Fig. 5D**). NAP not only improved the microtubular network but also the mitochondrial distribution and interconnectivity. Although with minor differences between chronic and acute models, together these data suggest that mitochondrial impairment leads to alterations in the autophagy system, as mainly translated by a reduction in the autophagic flux and that this is due to alterations in microtubule-dependent traffic.

4. Discussion

In this study we show that the repair of microtubule assembly prevents the accumulation of PD neuropathological hallmarks in cells with mitochondrial deficits. We present evidence that NAP, a microtubule stabilizing peptide, improves microtubule network assembly and so boosts mitochondrial trafficking and autophagic flux, restores mitochondrial membrane potential and reduces ASYN oligomers accumulation.

Several studies place mitochondrial dysfunction as the triggering event leading to the subsequent pathological hallmarks in PD **[71]**. Moreover, microtubule disorganization has also been shown to occur in PD. Indeed, two mitochondrial toxins widely used to model PD have been shown to affect microtubule

dynamics **[72-74]**. Previous work from our group demonstrated that sPD cybrids with a complex I defect, ATP depletion and loss of mitochondrial membrane potential **[18]** have a disorganized microtubule network **[22]**. An impaired microtubule-dependent traffic can compromise the movement of mitochondria, protein aggregates and autophagic vacuoles. This will in turn contribute to an accumulation of autophagosomes, defective mitochondria and protein oligomers leading to cell toxicity. In fact, in our previous work we also observed that ASYN oligomers accumulate in PD cybrids **[22]**.

Herein, our major goal was to assess if the modulation of microtubule network could be a feasible therapeutic target to PD. For this purpose we used an *ex-vivo* model, CT and sPD cybrids that share the same nuclear background but different mitochondrial background and an *in-vitro* model, cortical neurons exposed to MPP^+, a metabolite of 1-methyl-4-phenyl-1,2,3,6-tetrahydropyridine that was shown to induce Parkinsonism in humans, primates, and mice **[1]**.

To modulate microtubule network, we used NAP (1 nM in cybrid cells and 10 nM in cortical neurons exposed to MPP^+), an eight amino acid peptide, derived from activity-dependent neuroprotective protein, a molecule that is essential for brain formation **[75, 76]**. The fundamental mechanism for NAP protection is its interaction with the microtubule cytoskeleton, protecting microtubule function. In fact, NAP preferentially interacts with neuronal and glial tubulin and enhances proper microtubule assembly leading to increased cellular survival **[77]**. Despite previous data demonstrated that EpotiloneD and Taxol, two known antitumor drugs used to fight cancer, can be used as a neuroprotective strategy in Alzheimer's and Parkinson's disease models **[22, 78, 79]** we choose NAP peptide because it penetrates cells and crosses the blood-barrier after nasal or systematic administration, which makes it into a promising therapeutic molecule **[80]**. NAP has been shown to provide neuroprotection, *in vivo* and *in vitro* in several disease models **[81-83]** including Alzheimer's disease models **[84-87]**. Intranasal administration of NAP in mice overexpressing ASYN, improved motor function and reduced ASYN pathology **[88]**. Mechanistically, NAP was shown to prevent mitochondrial cytochrome c release in parallel with protection of the microtubule network **[89]**, connecting mitochondrial function to microtubule assembly as observed here.

Microtubules are highly stable and post-translational modifications such as acetylation of α-tubulin play a role in the maintenance of stable populations of microtubules **[90, 91]**. Accordingly, we observed a decrease in α-tubulin acetylation in sPD cybrids, which indicates microtubule instability. Most interestingly, we found that NAP increased the α-tubulin acetylation levels thereby improving microtubule assembly. These results were further confirmed in cortical neurons where α-tubulin acetylation decreased after MPP^+ exposure and was reversed following NAP treatment. Microtubular acetylation has been shown to cause the recruitment of molecular motors dyneins and kinesins to microtubules therefore possessing a role not only for the kinesin-dependent anterograde trafficking but also for the dynein-dependent retrograde trafficking of either lysosomes or autophagosomes **[92, 93].** Recent work from Xie and colleagues revealed that acetylated microtubules are required for fusion of autophagosomes with lysosomes **[94]**. Hence NAP, by increasing α-tubulin acetylation, can also promote the fusion of autophagosomes and lysosomes and subsequently improve autophagic degradation of its substrates. Indeed, we observed that NAP increased autophagosome-lysosome fusion in sPD cybrids. Besides, autophagosomes move along microtubules, they facilitate autophagosome formation and are

required to direct dispatch autophagosomes for degradation **[51, 52]**. Nocodazole, a known microtubule depolymerising agent, was shown to inhibit lysosomes fusion with autophagosomes resulting in an inefficient degradation of autophagic substrates **[95]**. Here, NAP protected against nocodazole-induced microtubule disassembly, corroborating and extending previous observations **[48]**. In our previous work we observed that LC3II levels were increased in sPD cybrids relatively to CT cybrids and that this was due to reduced rate of LC3II-associated autophagosomes clearance **[40]**. Given the fact that microtubules are responsible for axonal transport of organelles and vesicles, we decided to study whether NAP, by promoting microtubules assembly, probably due to increasing α-tubulin acetylation, would also restore the autophagic flux, so potentiating autophagosomal degradation. We observed that NAP promoted autophagosomal clearance in sPD cybrids comparatively to untreated sPD cybrids. Additionally, we observed an increase in autophagic flux in MPP^+-exposed neurons after NAP treatment, which supports our cybrid data. Interestingly, rapamycin, a classic activator of autophagy, was not able to increase the autophagic flux in sPD cybrids despite an increase in LC3II levels. These results further corroborate that autophagic induction is not compromised in sPD cybrids cells and that autophasosomal clearance failure is due to a defect in the microtubule-dependent intracellular traffic. Moreover, our previous results showed that rapamycin-induced autophagy did not prevent caspase-3 activation in sPD cybrids showing no protective effect **[40]**.

Mitochondria is one of the main substrates for autophagy **[96]** and recent works have linked defects in mitophagy to PD. Parkin and Pink1, two genes that are mutated in autosomal recessive PD, have been shown to play a role in mitophagy. Pink1, a mitochondrial kinase known to function upstream of parkin, accumulates in dysfunctional mitochondria upon loss of mitochondrial membrane potential, and this accumulation leads to mitochondrial parkin recruitment. Parkin once in the mitochondria triggers the assembly of p62 onto mitochondria by ubiquitination of VDAC1 and promotes mitochondrial fission by ubiquitination of mitofusins **[63, 59, 97]**. Eventually, after fragmentation of the mitochondrial pool, damaged mitochondria are surrounded selectively by autophagosomal membrane via p62–LC3 interaction **[64]**. Indeed we observed an increase in mitochondrial fragmentation in our sPD cybrids and in MPP^+-treated neurons. Despite this, a sustained increase in mitochondrial protein ubiquitination levels and a decrease in mitochondrial membrane potential is still observed in our sPD cells. We correlate these observations with the reduction of autophagic flux that do not allow for the removal of damaged mitochondria, despite the activation and formation of autophagosomes. It has been described that a failure in mitochondrial trafficking, similar to what we observed in sPD cybrids, induces a mitochondrial perinuclear distribution and an increase in mitochondrial fragmentation **[98, 99]**. Interestingly, we observed that in the sPD cybrids, NAP restored mitochondrial trafficking and distribution and promoted mitochondrial elongation and interconnectivity. Further validating this data we also observed that NAP promoted the assembly of βIII-Tubulin network, as well as, mitochondrial distribution and interconnectivity in MPP^+-treated cortical neurons. Gomes and co-workers reported that elongated mitochondria possess more cristae and increased ATP synthase activity, allowing the maintenance of ATP levels **[100]**. NAP, by improving tubulin-dependent traffic facilitates damaged mitochondria clearance by autophagy, which potentiates the maintenance of a healthy mitochondrial pool. Moreover, mitochondrial distribution and recruitment to localized areas with increased energy or calcium buffering

requirements make mitochondrial movement an important ongoing and regulated process **[101, 102]**. In our work mitochondrial deficient cells show a decrease in mitochondrial movement that was abolished by NAP treatment. More interestingly, we found that NAP decreases mitochondrial ubiquitination, restores mitochondrial membrane potential in sPD cybrids and reduces mitochondrial ASYN accumulation in sPD cybrids suggesting that damaged mitochondria are being cleared by autophagy. These results, together with the fact that NAP elongates mitochondria, show that NAP by recovering microtubule dependent traffic efficiently start a positive feedback loop where damaged mitochondria are degraded, healthy mitochondria survive and mitochondrial normal metabolism is restored.

ASYN is degraded by both autophagy and proteasome **[103].** However, ASYN oligomers block both chaperone mediated autophagy and proteosomal function. So, in situations where ASYN undergoes post-translational modifications, is oxidized or oligomerized it can only be degraded by macroautophagy **[104-107]**. Furthermore, transport of ASYN requires an intact microtubule network and involves kinesin and dynein motor proteins. **[108].** Li and colleagues results indicated that ASYN transport slows with aging **[54]**. This may lead to longer half-life of ASYN allowing greater opportunities for aggregation-promoting modifications, such as protein oxidation **[109-111, 19]**. Therefore, the age-associated changes in ASYN transport may contribute to the axonal ASYN abnormalities associated with alpha-synucleinopathies. Our previous work showed that microtubule destabilization driven by mitochondrial damage and deficient ATP supply leads to ASYN oligomerization **[22]**. Herein we demonstrate that NAP-treated cybrids have a reduction in ASYN oligomers, which is probably due to their degradation, either alone or together with mitochondria by autophagy. Moreover, the enhancement of ASYN traffic diminishes ASYN monomers opportunity to react with ROS **[19]** or calpains **[50]** reducing its capacity to oligomerize and to accumulate. Indeed, NAP also reduces mitochondrial ASYN accumulation showing that or ASYN sequestered by mitochondria is cleared by mitophagy or ASYN probability to oligomerize and to be sequestered by mitochondria is reduced.

In this work, we show strong evidence that by inducing microtubule assembly we can protect PD cells from ASYN accumulation and damaged mitochondria deleterious effects. Thus, by recover the autophagic flux a subsequently reduction in ASYN oligomers accumulation and a decrease in damaged mitochondria build-up occurs. Therefore, NAP demonstrates a great potential to treat neurodegenerative disease like PD, hampering the appearance of typical pathological hallmarks. In this respect, NAP (davunetide) is currently in a pivotal clinical trial in progressive supranuclear palsy (www.allontherapeutics.com), a Parkinson like syndrome exhibiting microtubule and mitochondrial dysfunction **[112]**.

Acknowledgements

We are grateful to Dr Rosa Resende, Dr Luísa Cortes for technical support. Work in our laboratory is supported by funds from PTDC/SAU-NEU/102710/2008 to SM Cardoso. AR Esteves is supported by Post-Doctoral Fellowship (SFRH/BPD/75044/2010) from Portuguese Foundation for Science and Technology (FCT-MCTES, Portugal). We are grateful to Dr Russell H Swerdlow for providing the PD

patients samples. We are grateful to Allon Therapeutics for support Professor Illana Gozes (Lily and Avraham Gildor Chair for the Investigations of Growth Factors and Adams Super Center for Brain Studies, Tel Aviv University) serves a Director-Chief Scientific Officer at Allon Therapeutics Inc., that is developing davunetide.

Author Contributions

Conceived and designed the experiments: ARE, SMC. Performed the experiments: ARE. Analyzed the data: ARE, SMC. Wrote the paper: ARE, IG, SMC. Synthesized NAP peptide: IG.

References

[1]J.W. Langston, P. Ballard, J.W. Tetrud, I. Irwin, Chronic Parkinsonism in humans due to a product of meperidine-analog synthesis, Science 219 (1983) 979-980.
[2]W.D. Parker, Jr., S.J. Boyson, J.K. Parks, Abnormalities of the electron transport chain in idiopathic Parkinson's disease, Ann Neurol 26 (1989) 719-723.
[3]P.M. Abou-Sleiman, M.M. Muqit, N.W. Wood, Expanding insights of mitochondrial dysfunction in Parkinson's disease, Nat Rev Neurosci 7 (2006) 207-219.
[4]P.M. Keeney, J. Xie, R.A. Capaldi, J.P. Bennett, Jr., Parkinson's disease brain mitochondrial complex I has oxidatively damaged subunits and is functionally impaired and misassembled, J Neurosci 26 (2006) 5256-5264.
[5]H. Bernheimer, W. Birkmayer, O. Hornykiewicz, K. Jellinger, F. Seitelberger, Brain dopamine and the syndromes of Parkinson and Huntington. Clinical, morphological and neurochemical correlations, J Neurol Sci 20 (1973) 415-455.
[6]B. Lach, D. Grimes, B. Benoit, A. Minkiewicz-Janda, Caudate nucleus pathology in Parkinson's disease: ultrastructural and biochemical findings in biopsy material, Acta Neuropathol 83 (1992) 352-360.
[7]E. Bertrand, W. Lechowicz, E. Lewandowska, G.M. Szpak, J. Dymecki, E. Kosno-Kruszewska, T. Wierzba-Bobrowicz, Degenerative axonal changes in the hippocampus and amygdala in Parkinson's disease, Folia Neuropathol 41 (2003) 197-207.
[8]D.M. Arduino, A.R. Esteves, C.R. Oliveira, S.M. Cardoso, Mitochondrial metabolism modulation: a new therapeutic approach for Parkinson's disease, CNS Neurol Disord Drug Targets 9 (2010) 105-119.
[9]M. Tanaka, Y.M. Kim, G. Lee, E. Junn, T. Iwatsubo, M.M. Mouradian, Aggresomes formed by alpha-synuclein and synphilin-1 are cytoprotective, J Biol Chem 279 (2004) 4625-4631.
[10]M.R. Cookson, M. van der Brug, Cell systems and the toxic mechanism(s) of alpha-synuclein, Exp Neurol 209 (2008) 5-11.
[11]H.Y. Kim, M.K. Cho, A. Kumar, E. Maier, C. Siebenhaar, S. Becker, C.O. Fernandez, H.A. Lashuel, R. Benz, A. Lange, M. Zweckstetter, Structural properties of pore-forming oligomers of alpha-synuclein, J Am Chem Soc 131 (2009) 17482-17489.
[12]B. Winner, R. Jappelli, S.K. Maji, P.A. Desplats, L. Boyer, S. Aigner, C. Hetzer, T. Loher, M. Vilar, S. Campioni, C. Tzitzilonis, A. Soragni, S. Jessberger, H. Mira, A. Consiglio, E. Pham, E. Masliah, F.H. Gage, R. Riek, In vivo demonstration that alpha-synuclein oligomers are toxic, Proc Natl Acad Sci U S A 108 (2011) 4194-4199.
[13]R.L. Morris, P.J. Hollenbeck, Axonal transport of mitochondria along microtubules and F-actin in living vertebrate neurons, J Cell Biol 131 (1995) 1315-1326.
[14]L.A. Ligon, O. Steward, Role of microtubules and actin filaments in the movement of mitochondria in the axons and dendrites of cultured hippocampal neurons, J Comp Neurol 427 (2000) 351-361.
[15]H.J. Lee, F. Khoshaghideh, S. Lee, S.J. Lee, Impairment of microtubule-dependent trafficking by overexpression of alpha-synuclein, Eur J Neurosci 24 (2006) 3153-3162.

[16]G. Schiavo, M. Fainzilber, Cell biology: Alternative energy for neuronal motors, Nature 495 (2013) 178-180.
[17]D. Zala, M.V. Hinckelmann, H. Yu, M.M. Lyra da Cunha, G. Liot, F.P. Cordelieres, S. Marco, F. Saudou, Vesicular glycolysis provides on-board energy for fast axonal transport, Cell 152 (2013) 479-491.
[18]A.R. Esteves, A.F. Domingues, I.L. Ferreira, C. Januario, R.H. Swerdlow, C.R. Oliveira, S.M. Cardoso, Mitochondrial function in Parkinson's disease cybrids containing an nt2 neuron-like nuclear background, Mitochondrion 8 (2008) 219-228.
[19]A.R. Esteves, D.M. Arduino, R.H. Swerdlow, C.R. Oliveira, S.M. Cardoso, Oxidative stress involvement in alpha-synuclein oligomerization in Parkinson's disease cybrids, Antioxid Redox Signal 11 (2009) 439-448.
[20]A.R. Esteves, J. Lu, M. Rodova, I. Onyango, E. Lezi, R. Dubinsky, K.E. Lyons, R. Pahwa, J.M. Burns, S.M. Cardoso, R.H. Swerdlow, Mitochondrial respiration and respiration-associated proteins in cell lines created through Parkinson's subject mitochondrial transfer, J Neurochem 113 (2010) 674-682.
[21]R.H. Swerdlow, J.K. Parks, S.W. Miller, J.B. Tuttle, P.A. Trimmer, J.P. Sheehan, J.P. Bennett, Jr., R.E. Davis, W.D. Parker, Jr., Origin and functional consequences of the complex I defect in Parkinson's disease, Ann Neurol 40 (1996) 663-671.
[22]A.R. Esteves, D.M. Arduino, R.H. Swerdlow, C.R. Oliveira, S.M. Cardoso, Microtubule depolymerization potentiates alpha-synuclein oligomerization, Front Aging Neurosci 1 (2010) 5.
[23]J.J. Lee, S.M. Swain, Peripheral neuropathy induced by microtubule-stabilizing agents, J Clin Oncol 24 (2006) 1633-1642.
[24]M.L. Michaelis, G. Georg, H. Telikepalli, M. McIntosh, R.A. Rajewski, Ongoing in vivo studies with cytoskeletal drugs in tau transgenic mice, Curr Alzheimer Res 3 (2006) 215-219.
[25]M. Bassan, R. Zamostiano, A. Davidson, A. Pinhasov, E. Giladi, O. Perl, H. Bassan, C. Blat, G. Gibney, G. Glazner, D.E. Brenneman, I. Gozes, Complete sequence of a novel protein containing a femtomolar-activity-dependent neuroprotective peptide, J Neurochem 72 (1999) 1283-1293.
[26]R. Zamostiano, A. Pinhasov, E. Gelber, R.A. Steingart, E. Seroussi, E. Giladi, M. Bassan, Y. Wollman, H.J. Eyre, J.C. Mulley, D.E. Brenneman, I. Gozes, Cloning and characterization of the human activity-dependent neuroprotective protein, J Biol Chem 276 (2001) 708-714.
[27]I. Gozes, Activity-dependent neuroprotective protein: from gene to drug candidate, Pharmacol Ther 114 (2007) 146-154.
[28]I. Divinski, L. Mittelman, I. Gozes, A femtomolar acting octapeptide interacts with tubulin and protects astrocytes against zinc intoxication, J Biol Chem 279 (2004) 28531-28538.
[29]I. Gozes, I. Divinski, The femtomolar-acting NAP interacts with microtubules: Novel aspects of astrocyte protection, J Alzheimers Dis 6 (2004) S37-41.
[30]I. Divinski, M. Holtser-Cochav, I. Vulih-Schultzman, R.A. Steingart, I. Gozes, Peptide neuroprotection through specific interaction with brain tubulin, J Neurochem 98 (2006) 973-984.
[31]I. Litvan, Update on epidemiological aspects of progressive supranuclear palsy, Mov Disord 18 Suppl 6 (2003) S43-50.
[32]D. Krige, M.T. Carroll, J.M. Cooper, C.D. Marsden, A.H. Schapira, Platelet mitochondrial function in Parkinson's disease. The Royal Kings and Queens Parkinson Disease Research Group, Ann Neurol 32 (1992) 782-788.
[33]M.M. Bradford, A rapid and sensitive method for the quantitation of microgram quantities of protein utilizing the principle of protein-dye binding, Anal Biochem 72 (1976) 248-254.
[34]C. Sodja, H. Fang, T. Dasgupta, M. Ribecco, P.R. Walker, M. Sikorska, Identification of functional dopamine receptors in human teratocarcinoma NT2 cells, Brain Res Mol Brain Res 99 (2002) 83-91.
[35]I.E. Misiuta, S. Saporta, P.R. Sanberg, T. Zigova, A.E. Willing, Influence of retinoic acid and lithium on proliferation and dopaminergic potential of human NT2 cells, J Neurosci Res 83 (2006) 668-679.
[36]R.H. Swerdlow, J.K. Parks, D.S. Cassarino, D.J. Maguire, R.S. Maguire, J.P. Bennett, Jr., R.E. Davis, W.D. Parker, Jr., Cybrids in Alzheimer's disease: a cellular model of the disease?, Neurology 49 (1997) 918-925.
[37]D.R. Binder, W.H. Dunn, Jr., R.H. Swerdlow, Molecular characterization of mtDNA depleted and repleted NT2 cell lines, Mitochondrion 5 (2005) 255-265.
[38]S.M. Cardoso, A.C. Rego, N. Penacho, C.R. Oliveira, Apoptotic cell death induced by hydrogen peroxide in NT2 parental and mitochondrial DNA depleted cells, Neurochem Int 45 (2004) 693-698.

[39]S.W. Miller, P.A. Trimmer, W.D. Parker, Jr., R.E. Davis, Creation and characterization of mitochondrial DNA-depleted cell lines with "neuronal-like" properties, J Neurochem 67 (1996) 1897-1907.
[40]D.M. Arduino, A.R. Esteves, L. Cortes, D.F. Silva, B. Patel, M. Grazina, R.H. Swerdlow, C.R. Oliveira, S.M. Cardoso, Mitochondrial metabolism in Parkinson's disease impairs quality control autophagy by hampering microtubule-dependent traffic, Hum Mol Genet 21 (2012) 4680-4702.
[41]A.C. Yu, T.E. Fisher, E. Hertz, J.T. Tildon, A. Schousboe, L. Hertz, Metabolic fate of [14C]-glutamine in mouse cerebral neurons in primary cultures, J Neurosci Res 11 (1984) 351-357.
[42]R. Resende, E. Ferreiro, C. Pereira, C.R. Oliveira, ER stress is involved in Abeta-induced GSK-3beta activation and tau phosphorylation, J Neurosci Res 86 (2008) 2091-2099.
[43]H.C. Joshi, D.W. Cleveland, Differential utilization of beta-tubulin isotypes in differentiating neurites, J Cell Biol 109 (1989) 663-673.
[44]H. Du, L. Guo, S. Yan, A.A. Sosunov, G.M. McKhann, S.S. Yan, Early deficits in synaptic mitochondria in an Alzheimer's disease mouse model, Proc Natl Acad Sci U S A 107 (2010) 18670-18675.
[45]R.K. Dagda, S.J. Cherra, 3rd, S.M. Kulich, A. Tandon, D. Park, C.T. Chu, Loss of PINK1 function promotes mitophagy through effects on oxidative stress and mitochondrial fission, J Biol Chem 284 (2009) 13843-13855.
[46]S. Bolte, F.P. Cordelieres, A guided tour into subcellular colocalization analysis in light microscopy, J Microsc 224 (2006) 213-232.
[47]C. Janke, J.C. Bulinski, Post-translational regulation of the microtubule cytoskeleton: mechanisms and functions, Nat Rev Mol Cell Biol 12 (2011) 773-786.
[48]I. Gozes, I. Divinski, NAP, a neuroprotective drug candidate in clinical trials, stimulates microtubule assembly in the living cell, Curr Alzheimer Res 4 (2007) 507-509.
[49]A.F. MacAskill, J.T. Kittler, Control of mitochondrial transport and localization in neurons, Trends Cell Biol 20 (2010) 102-112.
[50]A.R. Esteves, D.M. Arduino, R.H. Swerdlow, C.R. Oliveira, S.M. Cardoso, Dysfunctional mitochondria uphold calpain activation: contribution to Parkinson's disease pathology, Neurobiol Dis 37 (2010) 723-730.
[51]E. Fass, E. Shvets, I. Degani, K. Hirschberg, Z. Elazar, Microtubules support production of starvation-induced autophagosomes but not their targeting and fusion with lysosomes, J Biol Chem 281 (2006) 36303-36316.
[52]R. Kochl, X.W. Hu, E.Y. Chan, S.A. Tooze, Microtubules facilitate autophagosome formation and fusion of autophagosomes with endosomes, Traffic 7 (2006) 129-145.
[53]M. Bains, K.A. Heidenreich, Live-cell imaging of autophagy induction and autophagosome-lysosome fusion in primary cultured neurons, Methods Enzymol 453 (2009) 145-158.
[54]W. Li, P.N. Hoffman, W. Stirling, D.L. Price, M.K. Lee, Axonal transport of human alpha-synuclein slows with aging but is not affected by familial Parkinson's disease-linked mutations, J Neurochem 88 (2004) 401-410.
[55]A.R. Saha, J. Hill, M.A. Utton, A.A. Asuni, S. Ackerley, A.J. Grierson, C.C. Miller, A.M. Davies, V.L. Buchman, B.H. Anderton, D.P. Hanger, Parkinson's disease alpha-synuclein mutations exhibit defective axonal transport in cultured neurons, J Cell Sci 117 (2004) 1017-1024.
[56]P.A. Parone, S. Da Cruz, D. Tondera, Y. Mattenberger, D.I. James, P. Maechler, F. Barja, J.C. Martinou, Preventing mitochondrial fission impairs mitochondrial function and leads to loss of mitochondrial DNA, PLoS One 3 (2008) e3257.
[57]K. Mopert, P. Hajek, S. Frank, C. Chen, J. Kaufmann, A. Santel, Loss of Drp1 function alters OPA1 processing and changes mitochondrial membrane organization, Exp Cell Res 315 (2009) 2165-2180.
[58]N. Matsuda, S. Sato, K. Shiba, K. Okatsu, K. Saisho, C.A. Gautier, Y.S. Sou, S. Saiki, S. Kawajiri, F. Sato, M. Kimura, M. Komatsu, N. Hattori, K. Tanaka, PINK1 stabilized by mitochondrial depolarization recruits Parkin to damaged mitochondria and activates latent Parkin for mitophagy, J Cell Biol 189 (2010) 211-221.
[59]D.P. Narendra, S.M. Jin, A. Tanaka, D.F. Suen, C.A. Gautier, J. Shen, M.R. Cookson, R.J. Youle, PINK1 is selectively stabilized on impaired mitochondria to activate Parkin, PLoS Biol 8 (2010) e1000298.
[60]C. Vives-Bauza, C. Zhou, Y. Huang, M. Cui, R.L. de Vries, J. Kim, J. May, M.A. Tocilescu, W. Liu, H.S. Ko, J. Magrane, D.J. Moore, V.L. Dawson, R. Grailhe, T.M. Dawson, C. Li, K. Tieu, S. Przedborski, PINK1-dependent recruitment of Parkin to mitochondria in mitophagy, Proc Natl Acad Sci U S A 107 (2010) 378-383.

[61]N.C. Chan, A.M. Salazar, A.H. Pham, M.J. Sweredoski, N.J. Kolawa, R.L. Graham, S. Hess, D.C. Chan, Broad activation of the ubiquitin-proteasome system by Parkin is critical for mitophagy, Hum Mol Genet 20 (2011) 1726-1737.

[62]J.Y. Grey, M.K. Connor, J.W. Gordon, M. Yano, M. Mori, D.A. Hood, Tom20-mediated mitochondrial protein import in muscle cells during differentiation, Am J Physiol Cell Physiol 279 (2000) C1393-1400.

[63]D. Narendra, A. Tanaka, D.F. Suen, R.J. Youle, Parkin is recruited selectively to impaired mitochondria and promotes their autophagy, J Cell Biol 183 (2008) 795-803.

[64]S. Geisler, K.M. Holmstrom, D. Skujat, F.C. Fiesel, O.C. Rothfuss, P.J. Kahle, W. Springer, PINK1/Parkin-mediated mitophagy is dependent on VDAC1 and p62/SQSTM1, Nat Cell Biol 12 (2010) 119-131.

[65]D. Narendra, L.A. Kane, D.N. Hauser, I.M. Fearnley, R.J. Youle, p62/SQSTM1 is required for Parkin-induced mitochondrial clustering but not mitophagy; VDAC1 is dispensable for both, Autophagy 6 (2010) 1090-1106.

[66]L. Devi, V. Raghavendran, B.M. Prabhu, N.G. Avadhani, H.K. Anandatheerthavarada, Mitochondrial import and accumulation of alpha-synuclein impair complex I in human dopaminergic neuronal cultures and Parkinson disease brain, J Biol Chem 283 (2008) 9089-9100.

[67]M.S. Parihar, A. Parihar, M. Fujita, M. Hashimoto, P. Ghafourifar, Mitochondrial association of alpha-synuclein causes oxidative stress, Cell Mol Life Sci 65 (2008) 1272-1284.

[68]S.J. Chinta, J.K. Mallajosyula, A. Rane, J.K. Andersen, Mitochondrial alpha-synuclein accumulation impairs complex I function in dopaminergic neurons and results in increased mitophagy in vivo, Neurosci Lett 486 (2010) 235-239.

[69]A.F. Domingues, A.R. Esteves, R.H. Swerdlow, C.R. Oliveira, S.M. Cardoso, Calpain-mediated MPP+ toxicity in mitochondrial DNA depleted cells, Neurotox Res 13 (2008) 31-38.

[70]D. Cartelli, C. Ronchi, M.G. Maggioni, S. Rodighiero, E. Giavini, G. Cappelletti, Microtubule dysfunction precedes transport impairment and mitochondria damage in MPP+ -induced neurodegeneration, J Neurochem 115 (2010) 247-258.

[71]S.M. Cardoso, The mitochondrial cascade hypothesis for Parkinson's disease, Curr Pharm Des 17 (2011) 3390-3397.

[72]G. Cappelletti, T. Surrey, R. Maci, The parkinsonism producing neurotoxin MPP+ affects microtubule dynamics by acting as a destabilising factor, FEBS Lett 579 (2005) 4781-4786.

[73]G. Morfini, G. Pigino, K. Opalach, Y. Serulle, J.E. Moreira, M. Sugimori, R.R. Llinas, S.T. Brady, 1-Methyl-4-phenylpyridinium affects fast axonal transport by activation of caspase and protein kinase C, Proc Natl Acad Sci U S A 104 (2007) 2442-2447.

[74]Y. Ren, J. Feng, Rotenone selectively kills serotonergic neurons through a microtubule-dependent mechanism, J Neurochem 103 (2007) 303-311.

[75]A. Pinhasov, S. Mandel, A. Torchinsky, E. Giladi, Z. Pittel, A.M. Goldsweig, S.J. Servoss, D.E. Brenneman, I. Gozes, Activity-dependent neuroprotective protein: a novel gene essential for brain formation, Brain Res Dev Brain Res 144 (2003) 83-90.

[76]I. Gozes, B.H. Morimoto, J. Tiong, A. Fox, K. Sutherland, D. Dangoor, M. Holser-Cochav, K. Vered, P. Newton, P.S. Aisen, Y. Matsuoka, C.H. van Dyck, L. Thal, NAP: research and development of a peptide derived from activity-dependent neuroprotective protein (ADNP), CNS Drug Rev 11 (2005) 353-368.

[77]I. Gozes, R.A. Steingart, A.D. Spier, NAP mechanisms of neuroprotection, J Mol Neurosci 24 (2004) 67-72.

[78]B. Zhang, J. Carroll, J.Q. Trojanowski, Y. Yao, M. Iba, J.S. Potuzak, A.M. Hogan, S.X. Xie, C. Ballatore, A.B. Smith, 3rd, V.M. Lee, K.R. Brunden, The microtubule-stabilizing agent, epothilone D, reduces axonal dysfunction, neurotoxicity, cognitive deficits, and Alzheimer-like pathology in an interventional study with aged tau transgenic mice, J Neurosci 32 (2012) 3601-3611.

[79]D. Cartelli, F. Casagrande, C.L. Busceti, D. Bucci, G. Molinaro, A. Traficante, D. Passarella, E. Giavini, G. Pezzoli, G. Battaglia, G. Cappelletti, Microtubule alterations occur early in experimental parkinsonism and the microtubule stabilizer epothilone D is neuroprotective, Sci Rep 3 (2013) 1837.

[80]I. Gozes, I. Divinsky, I. Pilzer, M. Fridkin, D.E. Brenneman, A.D. Spier, From vasoactive intestinal peptide (VIP) through activity-dependent neuroprotective protein (ADNP) to NAP: a view of neuroprotection and cell division, J Mol Neurosci 20 (2003) 315-322.

[81]R.R. Leker, A. Teichner, N. Grigoriadis, H. Ovadia, D.E. Brenneman, M. Fridkin, E. Giladi, J. Romano, I. Gozes, NAP, a femtomolar-acting peptide, protects the brain against ischemic injury by reducing apoptotic death, Stroke 33 (2002) 1085-1092.

[82]T. Jehle, C. Dimitriu, S. Auer, R. Knoth, M. Vidal-Sanz, I. Gozes, W.A. Lagreze, The neuropeptide NAP provides neuroprotection against retinal ganglion cell damage after retinal ischemia and optic nerve crush, Graefes Arch Clin Exp Ophthalmol 246 (2008) 1255-1263.
[83]A. Idan-Feldman, Y. Schirer, E. Polyzoidou, O. Touloumi, R. Lagoudaki, N.C. Grigoriadis, I. Gozes, Davunetide (NAP) as a preventative treatment for central nervous system complications in a diabetes rat model, Neurobiol Dis 44 (2011) 327-339.
[84]O. Ashur-Fabian, Y. Segal-Ruder, E. Skutelsky, D.E. Brenneman, R.A. Steingart, E. Giladi, I. Gozes, The neuroprotective peptide NAP inhibits the aggregation of the beta-amyloid peptide, Peptides 24 (2003) 1413-1423.
[85]Y. Matsuoka, A.J. Gray, C. Hirata-Fukae, S.S. Minami, E.G. Waterhouse, M.P. Mattson, F.M. LaFerla, I. Gozes, P.S. Aisen, Intranasal NAP administration reduces accumulation of amyloid peptide and tau hyperphosphorylation in a transgenic mouse model of Alzheimer's disease at early pathological stage, J Mol Neurosci 31 (2007) 165-170.
[86]I. Gozes, I. Divinski, I. Piltzer, NAP and D-SAL: neuroprotection against the beta amyloid peptide (1-42), BMC Neurosci 9 Suppl 3 (2008) S3.
[87]N. Shiryaev, Y. Jouroukhin, E. Giladi, E. Polyzoidou, N.C. Grigoriadis, H. Rosenmann, I. Gozes, NAP protects memory, increases soluble tau and reduces tau hyperphosphorylation in a tauopathy model, Neurobiol Dis 34 (2009) 381-388.
[88]S.M. Fleming, C.K. Mulligan, F. Richter, F. Mortazavi, V. Lemesre, C. Frias, C. Zhu, A. Stewart, I. Gozes, B. Morimoto, M.F. Chesselet, A pilot trial of the microtubule-interacting peptide (NAP) in mice overexpressing alpha-synuclein shows improvement in motor function and reduction of alpha-synuclein inclusions, Mol Cell Neurosci 46 (2011) 597-606.
[89]I. Zemlyak, R. Sapolsky, I. Gozes, NAP protects against cytochrome c release: inhibition of the initiation of apoptosis, Eur J Pharmacol 618 (2009) 9-14.
[90]M.A. Cambray-Deakin, R.D. Burgoyne, Acetylated and detyrosinated alpha-tubulins are co-localized in stable microtubules in rat meningeal fibroblasts, Cell Motil Cytoskeleton 8 (1987) 284-291.
[91]M.A. Cambray-Deakin, R.D. Burgoyne, Posttranslational modifications of alpha-tubulin: acetylated and detyrosinated forms in axons of rat cerebellum, J Cell Biol 104 (1987) 1569-1574.
[92]J.C. Bulinski, Microtubule modification: acetylation speeds anterograde traffic flow, Curr Biol 17 (2007) R18-20.
[93]J.P. Dompierre, J.D. Godin, B.C. Charrin, F.P. Cordelieres, S.J. King, S. Humbert, F. Saudou, Histone deacetylase 6 inhibition compensates for the transport deficit in Huntington's disease by increasing tubulin acetylation, J Neurosci 27 (2007) 3571-3583.
[94]R. Xie, S. Nguyen, W.L. McKeehan, L. Liu, Acetylated microtubules are required for fusion of autophagosomes with lysosomes, BMC Cell Biol 11 (2010) 89.
[95]Y. Yang, L.Q. Feng, X.X. Zheng, Microtubule and kinesin/dynein-dependent, bi-directional transport of autolysosomes in neurites of PC12 cells, Int J Biochem Cell Biol 43 (2011) 1147-1156.
[96]L. Liu, R. Xie, S. Nguyen, M. Ye, W.L. McKeehan, Robust autophagy/mitophagy persists during mitosis, Cell Cycle 8 (2009) 1616-1620.
[97]D. Santos, S.M. Cardoso, Mitochondrial dynamics and neuronal fate in Parkinson's disease, Mitochondrion 12 (2012) 428-437.
[98]O.M. de Brito, L. Scorrano, Mitofusin 2 tethers endoplasmic reticulum to mitochondria, Nature 456 (2008) 605-610.
[99]D.W. Hailey, A.S. Rambold, P. Satpute-Krishnan, K. Mitra, R. Sougrat, P.K. Kim, J. Lippincott-Schwartz, Mitochondria supply membranes for autophagosome biogenesis during starvation, Cell 141 (2010) 656-667.
[100]L.C. Gomes, G. Di Benedetto, L. Scorrano, During autophagy mitochondria elongate, are spared from degradation and sustain cell viability, Nat Cell Biol 13 (2011) 589-598.
[101]R.S. Stowers, L.J. Megeath, J. Gorska-Andrzejak, I.A. Meinertzhagen, T.L. Schwarz, Axonal transport of mitochondria to synapses depends on milton, a novel Drosophila protein, Neuron 36 (2002) 1063-1077.
[102]E.E. Glater, L.J. Megeath, R.S. Stowers, T.L. Schwarz, Axonal transport of mitochondria requires milton to recruit kinesin heavy chain and is light chain independent, J Cell Biol 173 (2006) 545-557.
[103]J.L. Webb, B. Ravikumar, J. Atkins, J.N. Skepper, D.C. Rubinsztein, Alpha-Synuclein is degraded by both autophagy and the proteasome, J Biol Chem 278 (2003) 25009-25013.
[104]A.M. Cuervo, L. Stefanis, R. Fredenburg, P.T. Lansbury, D. Sulzer, Impaired degradation of mutant alpha-synuclein by chaperone-mediated autophagy, Science 305 (2004) 1292-1295.
[105]M. Martinez-Vicente, Z. Talloczy, S. Kaushik, A.C. Massey, J. Mazzulli, E.V. Mosharov, R. Hodara, R. Fredenburg, D.C. Wu, A. Follenzi, W. Dauer, S. Przedborski, H. Ischiropoulos, P.T.

Lansbury, D. Sulzer, A.M. Cuervo, Dopamine-modified alpha-synuclein blocks chaperone-mediated autophagy, J Clin Invest 118 (2008) 777-788.
[106]N.Y. Zhang, Z. Tang, C.W. Liu, alpha-Synuclein protofibrils inhibit 26 S proteasome-mediated protein degradation: understanding the cytotoxicity of protein protofibrils in neurodegenerative disease pathogenesis, J Biol Chem 283 (2008) 20288-20298.
[107]E. Emmanouilidou, L. Stefanis, K. Vekrellis, Cell-produced alpha-synuclein oligomers are targeted to, and impair, the 26S proteasome, Neurobiol Aging 31 (2010) 953-968.
[108]M.A. Utton, W.J. Noble, J.E. Hill, B.H. Anderton, D.P. Hanger, Molecular motors implicated in the axonal transport of tau and alpha-synuclein, J Cell Sci 118 (2005) 4645-4654.
[109]B.I. Giasson, J.E. Duda, I.V. Murray, Q. Chen, J.M. Souza, H.I. Hurtig, H. Ischiropoulos, J.Q. Trojanowski, V.M. Lee, Oxidative damage linked to neurodegeneration by selective alpha-synuclein nitration in synucleinopathy lesions, Science 290 (2000) 985-989.
[110]J.M. Souza, B.I. Giasson, Q. Chen, V.M. Lee, H. Ischiropoulos, Dityrosine cross-linking promotes formation of stable alpha -synuclein polymers. Implication of nitrative and oxidative stress in the pathogenesis of neurodegenerative synucleinopathies, J Biol Chem 275 (2000) 18344-18349.
[111]E. Paxinou, Q. Chen, M. Weisse, B.I. Giasson, E.H. Norris, S.M. Rueter, J.Q. Trojanowski, V.M. Lee, H. Ischiropoulos, Induction of alpha-synuclein aggregation by intracellular nitrative insult, J Neurosci 21 (2001) 8053-8061.
[112]V. Ries, W.H. Oertel, G.U. Hoglinger, Mitochondrial dysfunction as a therapeutic target in progressive supranuclear palsy, J Mol Neurosci 45 (2011) 684-689.

Figure Legends

Figure 1. NAP restores microtubule network assembly in PD cells. **(A)** Western Blot analysis and respective densitometry showing that NAP (1 nM) decreases the free/polymerized α-tubulin ratio in sPD cybrids. The data show a representative blot of 5 different experiments. Data is reported as absolute values. **(B)** Immunocytochemistry staining α-tubulin showing that NAP (1 nM) prevented the formation of loose tubulin bundles observed in sPD cybrids cells (n=3). Respective α-tubulin fluorescence intensity was calculated after morphometric quantification of cells stained as the ones shown here. Data is reported as the fold increase over untreated CT cybrids. **(C)** Western Blot analysis and respective densitometry demonstrating that NAP (1 nM) promoted a significant increase in tubulin acetylation in sPD cybrids. The data show a representative blots of 4 different experiments. Data is reported as the fold increase over untreated CT cybrids. **(D)** Immunocytochemistry of acetylated-α-Tubulin showing NAP (1 nM) effect on acetylated-tubulin pattern (n=2). Respective acetylated-α-tubulin fluorescence intensity was calculated after morphometric quantification of cells stained as the ones shown here. Data is reported as the fold increase over untreated CT cybrids. * $p<0.05$, ** $p<0.01$ and *** $p<0.001$, significantly different when compared to CT cybrid; # $p<0.05$ and ### $p<0.001$, significantly different when compared to untreated PD cybrid (Bonferroni's t test; two-tailed unpaired Student's t-test). All the blots were reprobed for GAPDH to confirm equal protein loading.

Figure 2. NAP improves mitochondrial trafficking in PD cells. (A) Representative kymograph images of mitochondrial movement in CT and PD cybrid cells treated with NAP (1 nM). Scale bars: 5 μM. **(B)**

Average mitochondria trafficking velocity (μm/s) shows that NAP slightly increases sPD cybrids mitochondrial movements (n=5). **(C)** Number of movable mitochondria were compared with those of total mitochondria indicating that NAP increases the number of movable mitochondria in sPD cybrids (n=5). The data is representative of 5 experiments with duplicated samples. *p<0.05 significantly different when compared to CT cybrid; #p<0.05 significantly different when compared to untreated sPD cybrids. (Bonferroni's t test; two-tailed unpaired Student's t-test).

Figure 3. NAP promotes autophagic clearance in PD cells. (A) Immunoblot for endogenous LC3B from CT and PD cybrids treated with NAP (1 nM) with or without lysosomal inhibitors (NH_4Cl and Leupeptin, N/L) and respective quantification of autophagic vacuoles (AVs) levels. Values of LC3II in the absence of N/L represent the steady state AVs content. The blots were reprobed for α-tubulin to confirm equal protein loading. The data show a representative blot derived from 5 independent experiments. Data is reported as the fold increase over untreated CT cybrids. **(B)** Assessment of autophagic flux, calculated as the ratio of LC3II densitometric value of N/L treated samples over the corresponding untreated samples. NAP-treated PD cybrid cells showed an increase in autophagic flux. Data is reported as the fold increase over untreated CT cybrids. **(C)** Immunocytochemistry analysis of LC3B showing a reduction in LC3B dots in NAP-treated sPD cybrids when compared to untreated sPD cybrids (n=2). Scale bars: 20 μm. **(D)** LC3B fluorescence intensity was calculated after morphometric quantification of cells stained as the ones shown here. Data is reported as absolute values. **(E)** LC3B (green) and Lamp-1 (red) immunostaining of CT and sPD cybrids treated with NAP for 24 h. In the last 4 h, cells were co-treated with or without lysosomal inhibitors (N/L) (n=2). Scale bars: 20 μm. **(F)** Assessment of LC3B and Lamp-1 co-localization. Data is reported as % of co-localization between LC3B and Lamp-1 **(G)** Lamp-1 fluorescence intensity was calculated after morphometric quantification of cells stained as the ones shown here. Data is reported as absolute values. *p<0.05, **p<0.01 and *** p<0.001, significantly different when compared to untreated CT cybrid; #p<0.05, and ### p<0.001, significantly different when compared to untreated PD cybrid. &p<0.05, significantly different when compared to PD cybrid treated with NAP. (Bonferroni's t test; two-tailed unpaired Student's t-test).

Figure 4. NAP improves mitochondrial function through completion of autophagy. (A) Immunocytochemistry analysis of Tom20 showing that NAP (1 nM) restores mitochondria elongation and ameliorates mitochondrial distribution (n=3). Mitochondrial morphology was calculated after morphometric quantification of cells stained with Tom20 as the ones shown here. **(B)** Mitochondrial interconnectivity and **(C)** Mitochondrial elongation was assessed using an ImageJ macro. Data is reported as absolute values. N=3 with 10-20 cells analysed per condition per experiment. .**p<0.01; *** p<0.001 significantly different when compared to untreated CT cybrids; ##p<0.01; ###p<0.001, significantly different when compared to untreated sPD cybrids. (Bonferroni's t test). **(D)** Mitochondrial membrane potential was expressed as the percentage of rhodamine 123 retention relatively to untreated CT cybrids, with the mean ± SEM derived from 5 independent experiments.*p<0.05, significantly different when

compared to untreated CT cybrids; #p<0.05, significantly different when compared to untreated sPD cybrids. (Bonferroni's t test). **(E)** Western Blot analysis and respective densitometry of ubiquitinated proteins levels illustrating a decrease of total ubiquitin content in NAP-treated sPD cybrids in both cytosolic and mitochondrial fractions. Mitochondrial and cytosolic fractions were reprobed for Tom20 and α-tubulin, respectively in order to confirm fractions purity. Blots are representative of 3 experiments. Data is reported as the fold increase over untreated CT cybrids. *** p<0.001, significantly different when compared to untreated CT cybrid cytosolic fraction; #p<0.05, significantly different when compared to untreated CT cybrid mitochondrial fraction; $^{\varphi\varphi}$p<0.01, significantly different when compared to untreated PD cybrid cytosolic fraction; $^{\chi}$p<0.05, significantly different when compared to untreated PD cybrid mitochondrial fraction. **(F)** Western Blot analysis and densitometry of mitochondrial and cytosolic ASYN content, showing a reduction of both cytosolic and mitochondrial ASYN content after NAP treatment in sPD cybrids. Mitochondrial and cytosolic fractions were reprobed for Tom20 and α-tubulin respectively in order to confirm fractions purity. Blots are representative of 6 different experiments. Data is reported as the fold increase over untreated CT cybrids. *p<0.05, significantly different when compared to untreated CT cybrid cytosolic fraction; #p<0.05, significantly different when compared to untreated PD cybrid cytosolic fraction; $^{\varphi}$p<0.05, significantly different when compared to untreated PD cybrid mitochondrial fraction. (Bonferroni's t test; two-tailed unpaired Student's t-test).

Figure 5. NAP prevents MPP^+-induced autophagic impairments in primary cortical neurons. (A) Western Blot analysis of acetylated-alpha-tubulin levels and respective densitometry in MPP+-treated cortical neurons. The data show a representative blot from 3 different experiments. Data are reported as the fold increase over the untreated neurons values. The blots were reprobed for α-tubulin to confirm equal protein loading. **(B)** Western blot analysis of the expression of endogenous LC3B and respective densitometry. The data show a representative blot from 3 different experiments. Data are reported as the fold increase over the untreated neurons values. **(C)** Assessment of autophagic flux by inhibiting lysosomal function with NH_4Cl and Leupeptin. **(D)** Immunocytochemistry analysis of Tom20 staining showing NAP protection (10 nM) in MPP^+-treated primary cortical neurons (n=2). βIII-Tubulin staining was used as a neuronal marker. Scale bars: 20 μm. Mitochondrial elongation and Mitochondrial interconnectivity was assessed using an ImageJ macro. Data is reported as absolute values. 10 to 20 cells were analysed per condition per experiment. α-tubulin and acetylated-α-tubulin fluorescence intensity was calculated after morphometric quantification of cells stained as the ones shown here. Data are reported as the fold increase over the untreated neurons values. *p<0.05, **p<0.01 and ***p<0.001, significantly different when compared untreated neurons; #p<0.05, ##p<0.01 and ###p<0.001, significantly different when compared to MPP^+-exposed neurons. (Bonferroni's t test; two-tailed unpaired Student's t-test).

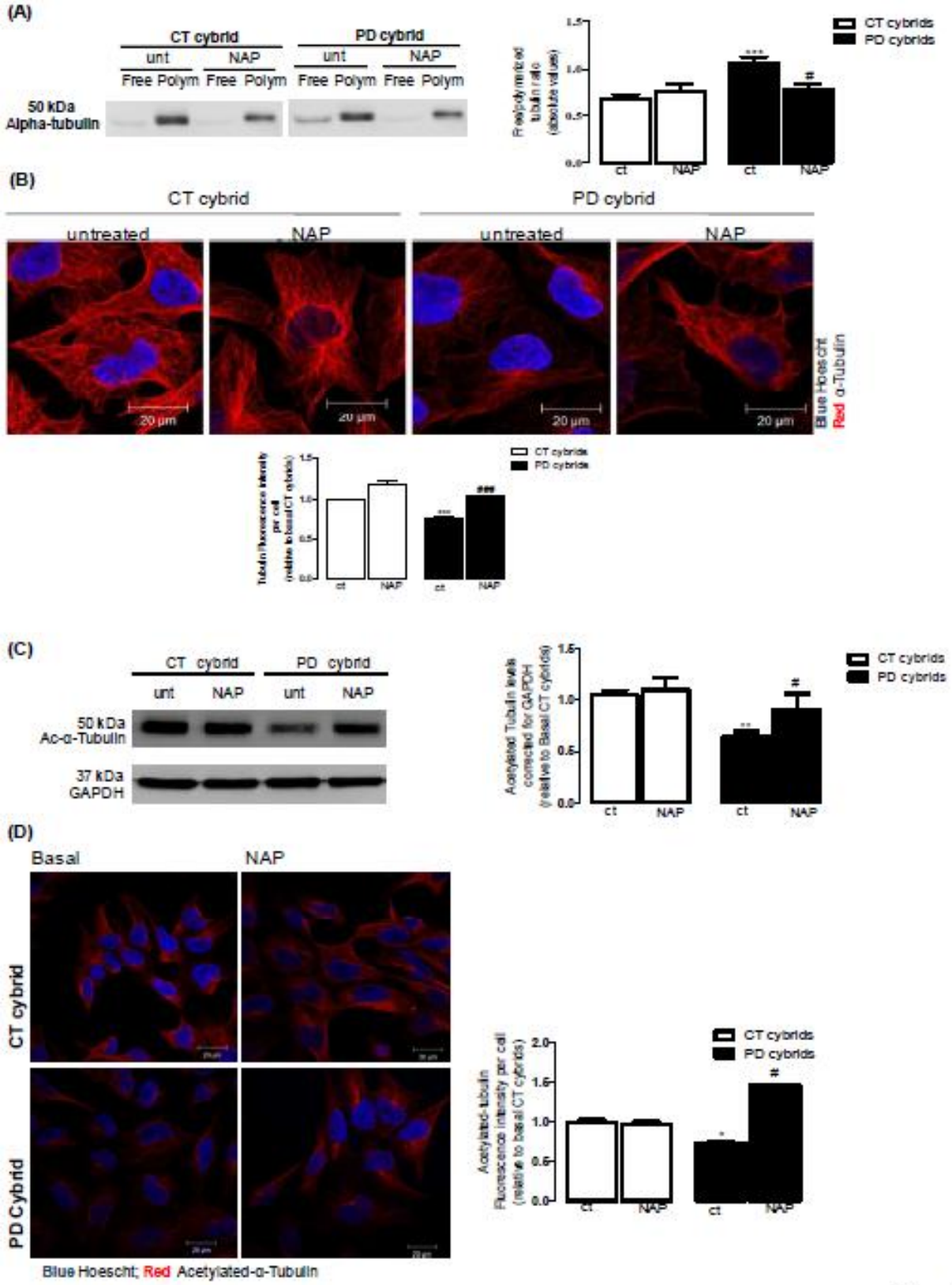
(A)
CT cybrid
PD cybrid
unt
NAP
Free Polym Free Polym Free Polym Free Polym
50 kDa
Alpha-tubulin
Polymerized tubulin ratio (absolute values)
CT cybrids
PD cybrids
ct
NAP
(B)
CT cybrid
PD cybrid
untreated
NAP
20 µm
Blue Hoescht
Red α-Tubulin
(C)
CT cybrid
PD cybrid
50 kDa
Ac-α-Tubulin
37 kDa
GAPDH
Acetylated Tubulin levels corrected for GAPDH (relative to Basal CT cybrids)
(D)
Basal
NAP
CT cybrid
PD Cybrid
Blue Hoescht; Red Acetylated-α-Tubulin
Acetylated-tubulin Fluorescence intensity per cell (relative to basal CT cybrids)

Figure 1

Figure 2

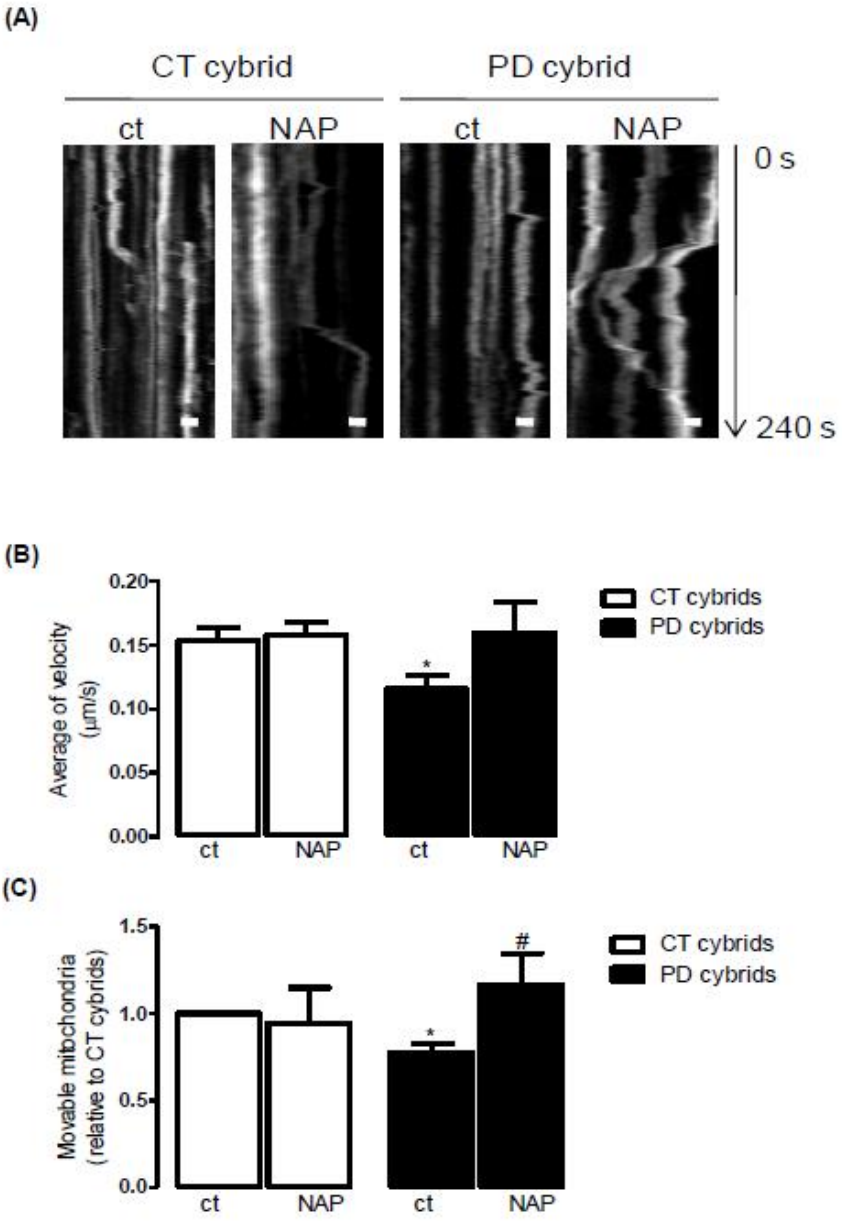

Figure 2

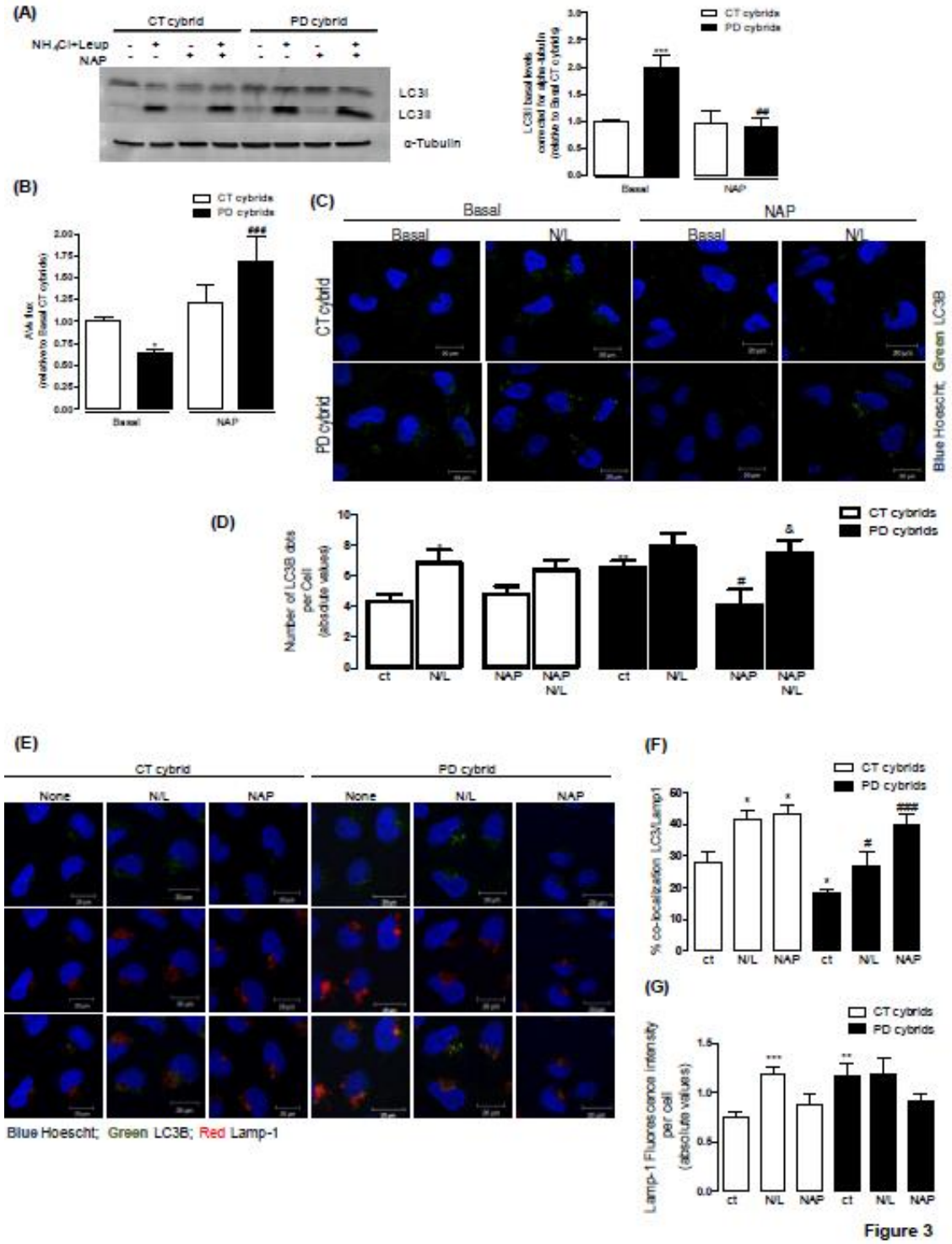

Figure 3

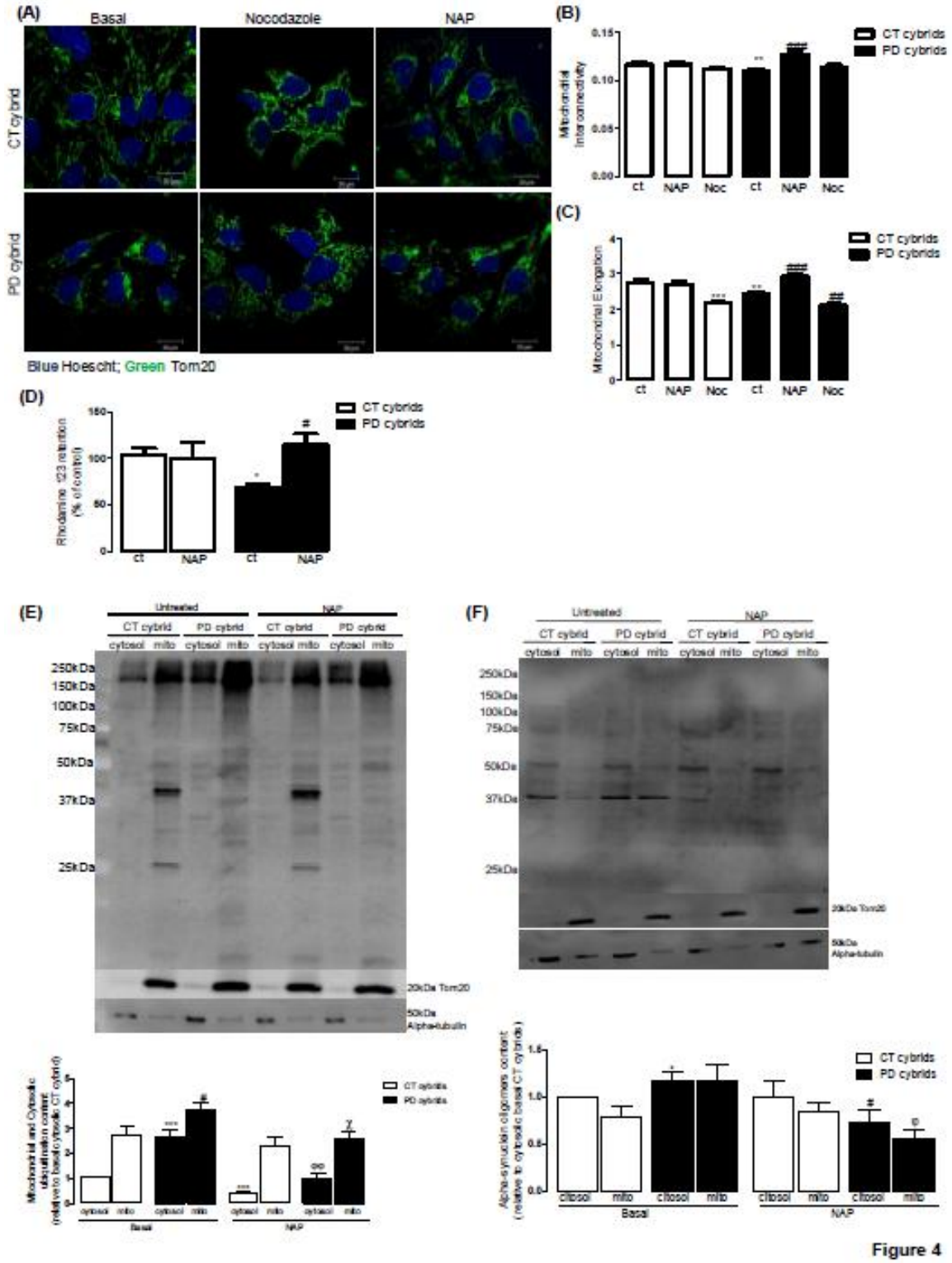
(A)
Basal
Nocodazole
NAP
CT cybrid
PD cybrid
Blue Hoescht; Green Tom20
(B)
CT cybrids
PD cybrids
Mitochondrial interconnectivity
ct
NAP
Noc
(C)
Mitochondrial Elongation
(D)
Rhodamine 123 retention (% of control)
(E)
Untreated
NAP
CT cybrid
PD cybrid
cytosol
mito
250kDa
150kDa
100kDa
75kDa
50kDa
37kDa
25kDa
20kDa Tom20
50kDa Alpha-tubulin
Basal
(F)
Alpha-synuclein oligomers content (relative to cytosolic basal CT cybrids)

Figure 4

Figure 5

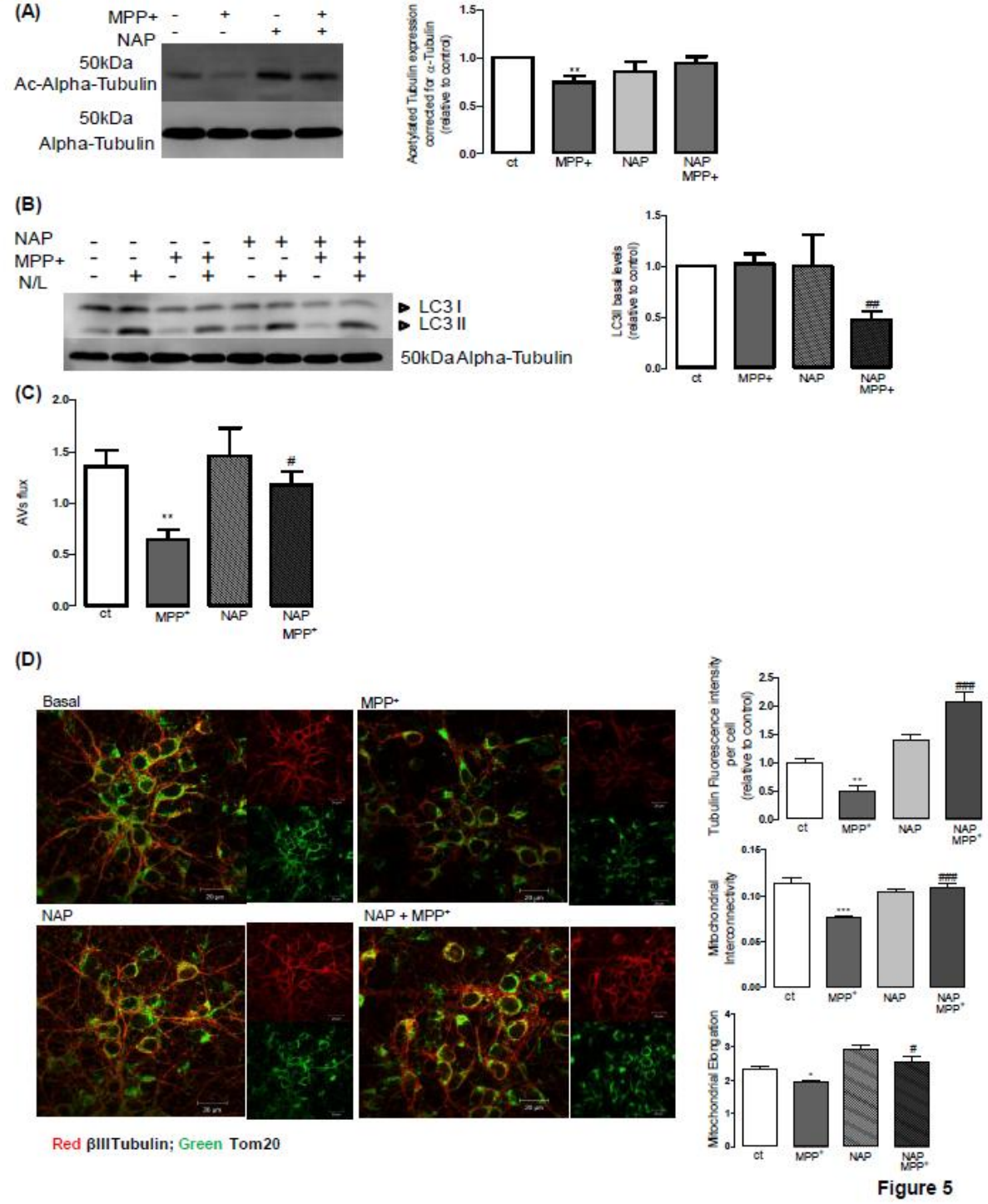

Figure 5

Highlights

- Damaged mitochondria induce microtubule disassembly.
- NAP improves microtubule network assembly and so boosts mitochondrial trafficking
- We show that NAP decreases ASYN accumulation and AVs accumulation.
- Microtubule assembly repair prevents the accumulation of PD pathological hallmarks
- Pharmacological stabilization of microtubules may be a viable strategy to treat PD